
8

Converter Transfer Functions

The engineering design process is comprised of several major steps:

1. *Specifications and other design goals* are defined.
2. *A circuit is proposed.* This is a creative process that draws on the physical insight and experience of the engineer.
3. *The circuit is modeled.* The converter power stage is modeled as described in Chapter 7. Components and other portions of the system are modeled as appropriate, often with vendor-supplied data.
4. *Design-oriented analysis* of the circuit is performed. This involves development of equations that allow element values to be chosen such that specifications and design goals are met. In addition, it may be necessary for the engineer to gain additional understanding and physical insight into the circuit behavior, so that the design can be improved by adding elements to the circuit or by changing circuit connections.
5. *Model verification.* Predictions of the model are compared to a laboratory prototype, under nominal operating conditions. The model is refined as necessary, so that the model predictions agree with laboratory measurements.
6. *Worst-case analysis* (or other reliability and production yield analysis) of the circuit is performed. This involves quantitative evaluation of the model performance, to judge whether specifications are met under all conditions. Computer simulation is well-suited to this task.
7. *Iteration.* The above steps are repeated to improve the design until the worst-case behavior meets specifications, or until the reliability and production yield are acceptably high.

This chapter covers techniques of design-oriented analysis, measurement of experimental transfer functions, and computer simulation, as needed in steps 4, 5, and 6.

Sections 8.1 to 8.3 discuss techniques for analysis and construction of the Bode plots of the converter transfer functions, input impedance, and output impedance predicted by the equivalent circuit

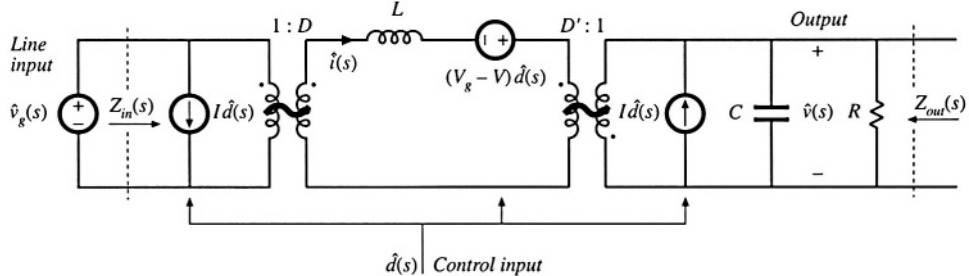


Fig. 8.1 Small-signal equivalent circuit model of the buck-boost converter, as derived in Chapter 7.

models of Chapter 7. For example, the small-signal equivalent circuit model of the buck-boost converter is illustrated in Fig. 7.17(c). This model is reproduced in Fig. 8.1, with the important inputs and terminal impedances identified. The line-to-output transfer function $G_{vg}(s)$ is found by setting duty cycle variations $\hat{d}(s)$ to zero, and then solving for the transfer function from $\hat{v}_g(s)$ to $\hat{v}(s)$:

$$G_{vg}(s) = \left. \frac{\hat{v}(s)}{\hat{v}_g(s)} \right|_{\hat{d}(s)=0} \quad (8.1)$$

This transfer function describes how variations or disturbances in the applied input voltage $v_g(t)$ lead to disturbances in the output voltage $v(t)$. It is important in design of an output voltage regulator. For example, in an off-line power supply, the converter input voltage $v_g(t)$ contains undesired even harmonics of the ac power line voltage. The transfer function $G_{vg}(s)$ is used to determine the effect of these harmonics on the converter output voltage $v(t)$.

The control-to-output transfer function $G_{vd}(s)$ is found by setting the input voltage variations $\hat{v}_g(s)$ to zero, and then solving the equivalent circuit model for $\hat{v}(s)$ as a function of $\hat{d}(s)$:

$$G_{vd}(s) = \left. \frac{\hat{v}(s)}{\hat{d}(s)} \right|_{\hat{v}_g(s)=0} \quad (8.2)$$

This transfer function describes how control input variations $\hat{d}(s)$ influence the output voltage $\hat{v}(s)$. In an output voltage regulator system, $G_{vd}(s)$ a key component of the loop gain and has a significant effect on regulator performance.

The output impedance $Z_{out}(s)$ is found under the conditions that $\hat{v}_g(s)$ and $\hat{d}(s)$ variations are set to zero. $Z_{out}(s)$ describes how variations in the load current affect the output voltage. This quantity is also important in voltage regulator design. It may be appropriate to define $Z_{out}(s)$ either including or not including the load resistance R .

The converter input impedance $Z_{in}(s)$ plays a significant role when an electromagnetic interference (EMI) filter is added at the converter power input. The relative magnitudes of Z_{in} and the EMI filter output impedance influence whether the EMI filter disrupts the transfer function $G_{vd}(s)$. Design of input EMI filters is the subject of Chapter 10.

An objective of this chapter is the construction of Bode plots of the important transfer functions and terminal impedances of switching converters. For example, Fig. 8.2 illustrates the magnitude and phase plots of $G_{vd}(s)$ for the buck-boost converter model of Fig. 8.1. Rules for construction of magnitude and phase asymptotes are reviewed in Section 8.1, including two types of features that often appear in

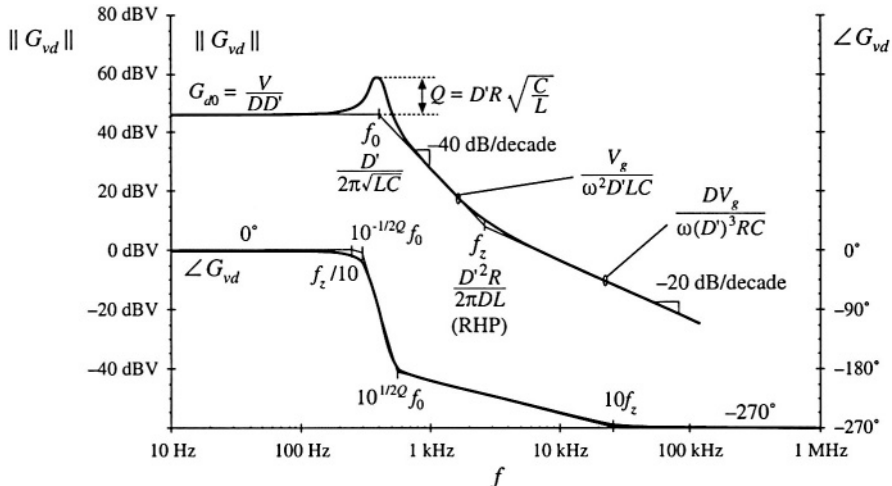


Fig. 8.2 Bode plot of control-to-output transfer function predicted by the model of Fig. 8.1, with analytical expressions for the important features.

converter transfer functions: resonances and right half-plane zeroes. Bode diagrams of the small-signal transfer functions of the buck-boost converter are derived in detail in Section 8.2, and the transfer functions of the basic buck, boost, and buck-boost converters are tabulated. The physical origins of the right half-plane zero are also described.

A difficulty usually encountered in circuit analysis (step 5 of the above list) is the complexity of the circuit model: practical circuits may contain hundreds of elements, and hence their analysis may lead to complicated derivations, intractable equations, and lots of algebra mistakes. *Design-oriented analysis*[1] is a collection of tools and techniques that can alleviate these problems. Some tools for approaching the design of a complicated converter system are described in this chapter. Writing the transfer functions in normalized form directly exposes the important features of the response. Analytical expressions for these features, as well as for the asymptotes, lead to simple equations that are useful in design. Well-separated roots of transfer function polynomials can be approximated in a simple way. Section 8.3 describes a graphical method for constructing Bode plots of transfer functions and impedances, essentially by inspection. This method can: (1) reduce the amount of algebra and associated algebra mistakes; (2) lead to greater insight into circuit behavior, which can be applied to design the circuit; and (3) lead to the insight necessary to make suitable approximations that render the equations tractable.

Experimental measurement of transfer functions and impedances (needed in step 4, model verification) is discussed in Section 8.5. Use of computer simulation to plot converter transfer functions (as needed in step 6, worst-case analysis) is covered in Appendix B.

8.1 REVIEW OF BODE PLOTS

A Bode plot is a plot of the magnitude and phase of a transfer function or other complex-valued quantity, vs. frequency. Magnitude in decibels, and phase in degrees, are plotted vs. frequency, using semilogarithmic axes. The magnitude plot is effectively a log-log plot, since the magnitude is expressed in decibels and the frequency axis is logarithmic.

The magnitude of a dimensionless quantity G can be expressed in decibels as follows:

$$\|G\|_{\text{dB}} = 20 \log_{10}(\|G\|) \quad (8.3)$$

Decibel values of some simple magnitudes are listed in Table 8.1. Care must be used when the magnitude is not dimensionless. Since it is not proper to take the logarithm of a quantity having dimensions, the magnitude must first be normalized. For example, to express the magnitude of an impedance Z in decibels, we should normalize by dividing by a base impedance R_{base} :

$$\|Z\|_{\text{dB}} = 20 \log_{10}\left(\frac{\|Z\|}{R_{\text{base}}}\right) \quad (8.4)$$

The value of R_{base} is arbitrary, but we need to tell others what value we have used. So if $\|Z\|$ is 5Ω , and we choose $R_{\text{base}} = 10 \Omega$, then we can say that $\|Z\|_{\text{dB}} = 20 \log_{10}(5 \Omega/10\Omega) = -6 \text{ dB}$ with respect to 10Ω . A common choice is $R_{\text{base}} = 1 \Omega$; decibel impedances expressed with $R_{\text{base}} = 1 \Omega$ are said to be expressed in $\text{dB}\Omega$. So 5Ω is equivalent to $14 \text{ dB}\Omega$. Current switching harmonics at the input port of a converter are often expressed in $\text{dB}\mu\text{A}$, or dB using a base current of $1 \mu\text{A}$: $60 \text{ dB}\mu\text{A}$ is equivalent to $1000 \mu\text{A}$, or 1 mA .

The magnitude Bode plots of functions equal to powers of f are linear. For example, suppose that the magnitude of a dimensionless quantity $G(f)$ is

$$\|G\| = \left(\frac{f}{f_0}\right)^n \quad (8.5)$$

where f_0 and n are constants. The magnitude in decibels is

$$\|G\|_{\text{dB}} = 20 \log_{10}\left(\frac{f}{f_0}\right)^n = 20n \log_{10}\left(\frac{f}{f_0}\right) \quad (8.6)$$

This equation is plotted in Fig. 8.3, for several values of n . The magnitudes have value 1 $\Rightarrow 0 \text{ dB}$ at frequency $f = f_0$. They are linear functions of $\log_{10}(f)$. The slope is the change in $\|G\|_{\text{dB}}$ arising from a unit change in $\log_{10}(f)$; a unit increase in $\log_{10}(f)$ corresponds to a factor of 10, or decade, increase in f . From Eq. (8.6), a decade increase in f leads to an increase in $\|G\|_{\text{dB}}$ of $20n \text{ dB}$. Hence, the slope is $20n \text{ dB}$ per decade. Equivalently, we can say that the slope is $20n \log_{10}(2) \approx 6n \text{ dB}$ per octave, where an octave is a factor of 2 change in frequency. In practice, the magnitudes of most frequency-dependent functions can usually be approximated over a limited range of frequencies by functions of the form (8.5); over this range of frequencies, the magnitude Bode plot is approximately linear with slope $20n \text{ dB}/\text{decade}$.

A simple transfer function whose magnitude is of the form (8.5) is the *pole at the origin*:

$$G(s) = \frac{1}{\left(\frac{s}{\omega_0}\right)} \quad (8.7)$$

The magnitude is

Table 8.1 Expressing magnitudes in decibels

Actual magnitude	Magnitude in dB
1/2	-6 dB
1	0 dB
2	6 dB
$5 = 10/2$	$20 \text{ dB} - 6 \text{ dB} = 14 \text{ dB}$
10	20 dB
$1000 = 10^3$	$3 \cdot 20 \text{ dB} = 60 \text{ dB}$

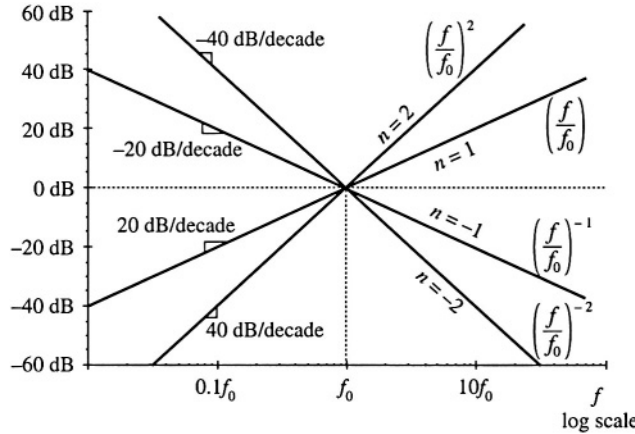


Fig. 8.3 Magnitude Bode plots of functions which vary as f^n are linear, with slope n dB per decade.

$$\|G(j\omega)\| = \left| \frac{1}{j\omega} \right| = \frac{1}{(\omega_0)} \quad (8.8)$$

If we define $f = \omega/2\pi$ and $f_0 = \omega_0/2\pi$, then Eq. (8.8) becomes

$$\|G\| = \left(\frac{f}{f_0} \right)^{-1} \quad (8.9)$$

which is of the form of Eq. (8.5) with $n = -1$. As illustrated in Fig. 8.3, the magnitude Bode plot of the pole at the origin (8.7) has a -20 dB per decade slope, and passes through 0 dB at frequency $f = f_0$.

8.1.1 Single Pole Response

Consider the simple R - C low-pass filter illustrated in Fig. 8.4. The transfer function is given by the voltage divider ratio

$$G(s) = \frac{v_2(s)}{v_1(s)} = \frac{\frac{1}{sC}}{\frac{1}{sC} + R} \quad (8.10)$$

This transfer function is a ratio of voltages, and hence is dimensionless. By multiplying the numerator and denominator by sC , we can express the transfer function as a rational fraction:

$$G(s) = \frac{1}{1 + sRC} \quad (8.11)$$

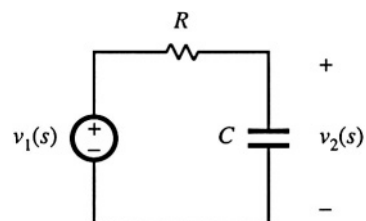


Fig. 8.4 Simple R - C low-pass filter example.

The transfer function now coincides with the following standard normalized form for a single pole:

$$G(s) = \frac{1}{1 + \frac{s}{\omega_0}} \quad (8.12)$$

The parameter $\omega_0 = 2\pi f_0$ is found by equating the coefficients of s in the denominators of Eqs. (8.11) and (8.12). The result is

$$\omega_0 = \frac{1}{RC} \quad (8.13)$$

Since R and C are real positive quantities, ω_0 is also real and positive. The denominator of Eq. (8.12) contains a root at $s = -\omega_0$, and hence $G(s)$ contains a real pole in the left half of the complex plane.

To find the magnitude and phase of the transfer function, we let $s = j\omega$, where j is the square root of -1 . We then find the magnitude and phase of the resulting complex-valued function. With $s = j\omega$, Eq. (8.12) becomes

$$G(j\omega) = \frac{1}{1 + j \frac{\omega}{\omega_0}} = \frac{1 - j \frac{\omega}{\omega_0}}{1 + \left(\frac{\omega}{\omega_0}\right)^2} \quad (8.14)$$

The complex-valued $G(j\omega)$ is illustrated in Fig. 8.5, for one value of ω . The magnitude is

$$\begin{aligned} \|G(j\omega)\| &= \sqrt{[\operatorname{Re}(G(j\omega))]^2 + [\operatorname{Im}(G(j\omega))]^2} \\ &= \frac{1}{\sqrt{1 + \left(\frac{\omega}{\omega_0}\right)^2}} \end{aligned} \quad (8.15)$$

Here, we have assumed that ω_0 is real. In decibels, the magnitude is

$$\|G(j\omega)\|_{dB} = -20 \log_{10} \left(\sqrt{1 + \left(\frac{\omega}{\omega_0}\right)^2} \right) \text{ dB} \quad (8.16)$$

The easy way to sketch the magnitude Bode plot of G is to investigate the asymptotic behavior for large and small frequency.

For small frequency, $\omega \ll \omega_0$ and $f \ll f_0$, it is true that

$$\left(\frac{\omega}{\omega_0}\right) \ll 1 \quad (8.17)$$

The $(\omega/\omega_0)^2$ term of Eq. (8.15) is therefore much smaller than 1, and hence Eq. (8.15) becomes

$$\|G(j\omega)\| \approx \frac{1}{\sqrt{1}} = 1 \quad (8.18)$$

In decibels, the magnitude is approximately

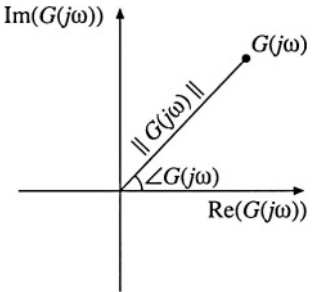


Fig. 8.5 Magnitude and phase of the complex-valued function $G(j\omega)$.

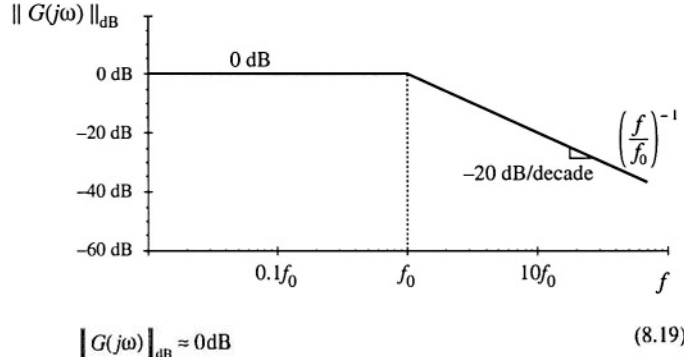


Fig. 8.6 Magnitude asymptotes for the single real pole transfer function.

Thus, as illustrated in Fig. 8.6, at low frequency $\| G(j\omega) \|_{\text{dB}}$ is asymptotic to 0 dB.

At high frequency, $\omega \gg \omega_0$ and $f \gg f_0$. In this case, it is true that

$$\left(\frac{\omega}{\omega_0} \right) \gg 1 \quad (8.20)$$

We can then say that

$$1 + \left(\frac{\omega}{\omega_0} \right)^2 \approx \left(\frac{\omega}{\omega_0} \right)^2 \quad (8.21)$$

Hence, Eq. (8.15) now becomes

$$\| G(j\omega) \| \approx \frac{1}{\sqrt{\left(\frac{\omega}{\omega_0} \right)^2}} = \left(\frac{f}{f_0} \right)^{-1} \quad (8.22)$$

This expression coincides with Eq. (8.5), with $n = -1$. So at high frequency, $\| G(j\omega) \|_{\text{dB}}$ has slope -20 dB per decade, as illustrated in Fig. 8.6. Thus, the asymptotes of $\| G(j\omega) \|$ are equal to 1 at low frequency, and $(f/f_0)^{-1}$ at high frequency. The asymptotes intersect at f_0 . The actual magnitude tends toward these asymptotes at very low frequency and very high frequency. In the vicinity of the corner frequency f_0 , the actual curve deviates somewhat from the asymptotes.

The deviation of the exact curve from the asymptotes can be found by simply evaluating Eq. (8.15). At the corner frequency $f = f_0$, Eq. (8.15) becomes

$$\| G(j\omega_0) \| = \frac{1}{\sqrt{1 + \left(\frac{\omega_0}{\omega_0} \right)^2}} = \frac{1}{\sqrt{2}} \quad (8.23)$$

In decibels, the magnitude is

$$\| G(j\omega_0) \|_{\text{dB}} = -20 \log_{10} \left(\sqrt{1 + \left(\frac{\omega_0}{\omega_0} \right)^2} \right) = -3 \text{ dB} \quad (8.24)$$

So the actual curve deviates from the asymptotes by -3 dB at the corner frequency, as illustrated in Fig. 8.7. Similar arguments show that the actual curve deviates from the asymptotes by -1 dB at $f = f_0/2$.

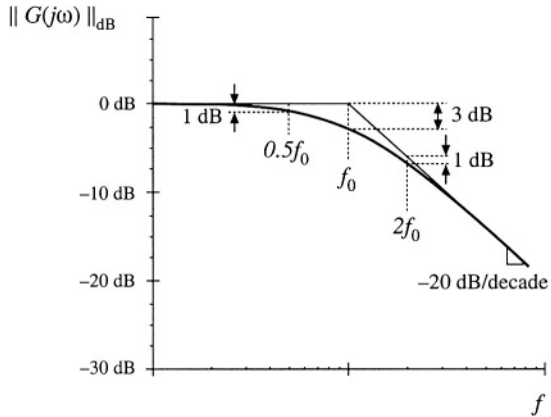


Fig. 8.7 Deviation of the actual curve from the asymptotes, real pole.

and at $f = 2f_0$.

The phase of $G(j\omega)$ is

$$\angle G(j\omega) = \tan^{-1} \left(\frac{\text{Im}(G(j\omega))}{\text{Re}(G(j\omega))} \right) \quad (8.25)$$

Insertion of the real and imaginary parts of Eq. (8.14) into Eq. (8.25) leads to

$$\angle G(j\omega) = -\tan^{-1} \left(\frac{\omega}{\omega_0} \right) \quad (8.26)$$

This function is plotted in Fig. 8.8. It tends to 0° at low frequency, and to -90° at high frequency. At the corner frequency $f = f_0$, the phase is -45° .

Since the high-frequency and low-frequency phase asymptotes do not intersect, we need a third asymptote to approximate the phase in the vicinity of the corner frequency f_0 . One way to do this is illus-

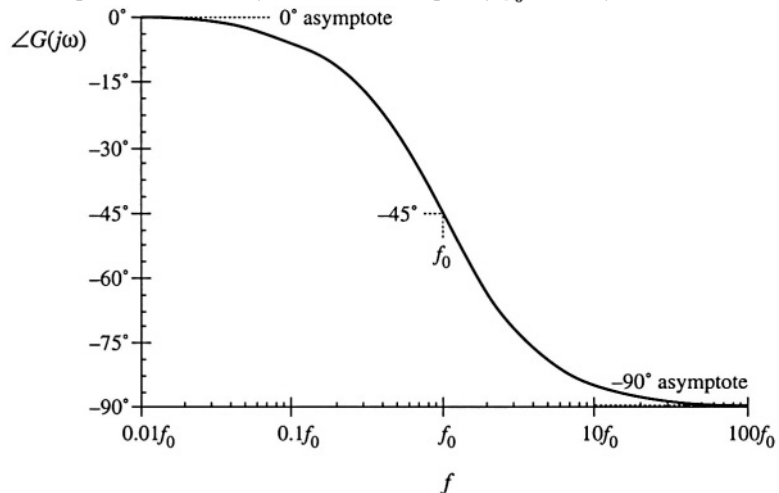


Fig. 8.8 Exact phase plot, single real pole.

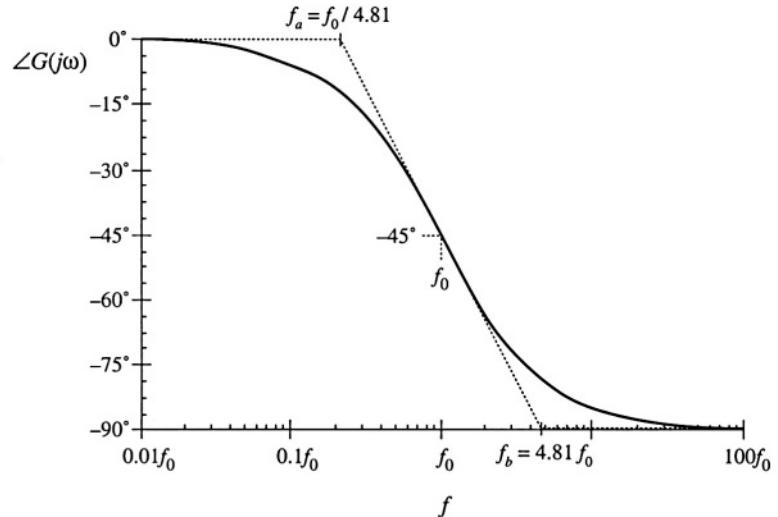


Fig. 8.9 One choice for the midfrequency phase asymptote, which correctly predicts the actual slope at $f = f_0$.

trated in Fig. 8.9, where the slope of the asymptote is chosen to be identical to the slope of the actual curve at $f = f_0$. It can be shown that, with this choice, the asymptote intersection frequencies f_a and f_b are given by

$$\begin{aligned} f_a &= f_0 e^{-\pi/2} \approx \frac{f_0}{4.81} \\ f_b &= f_0 e^{\pi/2} \approx 4.81 f_0 \end{aligned} \quad (8.27)$$

A simpler choice, which better approximates the actual curve, is

$$\begin{aligned} f_a &= \frac{f_0}{10} \\ f_b &= 10 f_0 \end{aligned} \quad (8.28)$$

This asymptote is compared to the actual curve in Fig. 8.10. The pole causes the phase to change over a frequency span of approximately two decades, centered at the corner frequency. The slope of the asymptote in this frequency span is -45° per decade. At the break frequencies f_a and f_b , the actual phase deviates from the asymptotes by $\tan^{-1}(0.1) = 5.7^\circ$.

The magnitude and phase asymptotes for the single-pole response are summarized in Fig. 8.11.

It is good practice to consistently express single-pole transfer functions in the normalized form of Eq. (8.12). Both terms in the denominator of Eq. (8.12) are dimensionless, and the coefficient of s^0 is unity. Equation (8.12) is easy to interpret, because of its normalized form. At low frequencies, where the (s/ω_0) term is small in magnitude, the transfer function is approximately equal to 1. At high frequencies, where the (s/ω_0) term has magnitude much greater than 1, the transfer function is approximately $(s/\omega_0)^{-1}$. This leads to a magnitude of $(f/f_0)^{-1}$. The corner frequency is $f_0 = \omega_0/2\pi$. So the transfer function is written directly in terms of its salient features, that is, its asymptotes and its corner frequency.

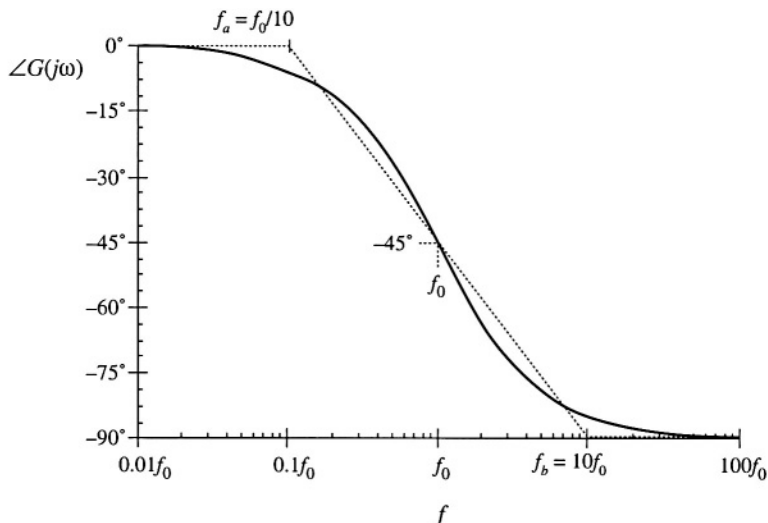


Fig. 8.10 A simpler choice for the midfrequency phase asymptote, which better approximates the curve over the entire frequency range.

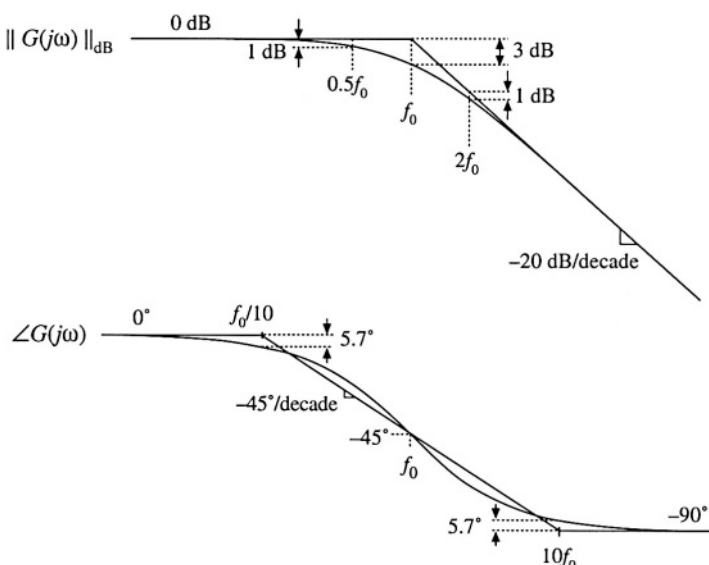


Fig. 8.11 Summary of the magnitude and phase Bode plot for the single real pole.

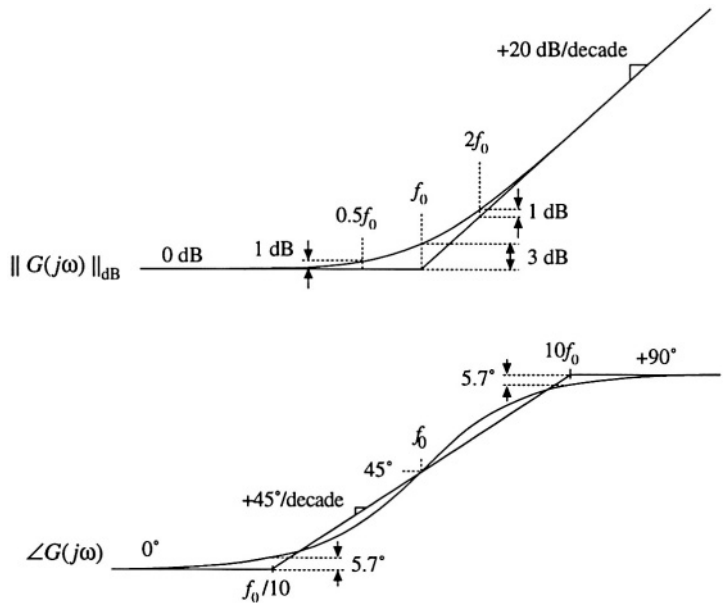


Fig. 8.12 Summary of the magnitude and phase Bode plot for the single real zero.

8.1.2 Single Zero Response

A single zero response contains a root in the numerator of the transfer function, and can be written in the following normalized form:

$$G(s) = \left(1 + \frac{s}{\omega_0} \right) \quad (8.29)$$

This transfer function has magnitude

$$\| G(j\omega) \| = \sqrt{1 + \left(\frac{\omega}{\omega_0} \right)^2} \quad (8.30)$$

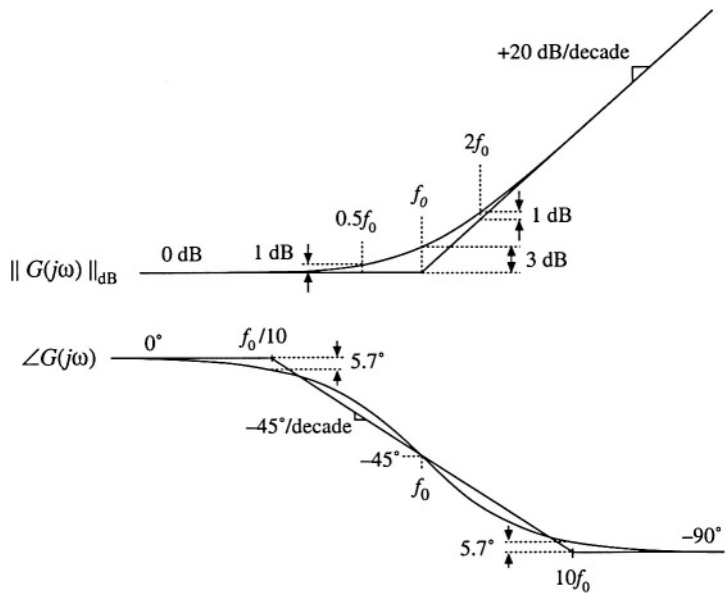
At low frequency, $f \ll f_0 = \omega_0/2\pi$, the transfer function magnitude tends to 1 $\Rightarrow 0$ dB. At high frequency, $f \gg f_0$, the transfer function magnitude tends to (f/f_0) . As illustrated in Fig. 8.12, the high-frequency asymptote has slope +20 dB/decade.

The phase is given by

$$\angle G(j\omega) = \tan^{-1} \left(\frac{\omega}{\omega_0} \right) \quad (8.31)$$

With the exception of a minus sign, the phase is identical to Eq. (8.26). Hence, suitable asymptotes are as illustrated in Fig. 8.12. The phase tends to 0° at low frequency, and to +90° at high frequency. Over the interval $f_0/10 < f < 10f_0$, the phase asymptote has a slope of +45°/decade.

Fig. 8.13 Summary of the magnitude and phase Bode plot for the real RHP zero.



8.1.3 Right Half-Plane Zero

Right half-plane zeroes are often encountered in the small-signal transfer functions of switching converters. These terms have the following normalized form:

$$G(s) = \left(1 - \frac{s}{\bar{\omega}_0}\right) \quad (8.32)$$

The root of Eq. (8.32) is positive, and hence lies in the right half of the complex s -plane. The right half-plane zero is also sometimes called a nonminimum phase zero. Its normalized form, Eq. (8.32), resembles the normalized form of the (left half-plane) zero of Eq. (8.29), with the exception of a minus sign in the coefficient of s . The minus sign causes a phase reversal at high frequency.

The transfer function has magnitude

$$|G(j\omega)| = \sqrt{1 + \left(\frac{\omega}{\bar{\omega}_0}\right)^2} \quad (8.33)$$

This expression is identical to Eq. (8.30). Hence, it is impossible to distinguish a right half-plane zero from a left half-plane zero by the magnitude alone. The phase is given by

$$\angle G(j\omega) = -\tan^{-1} \left(\frac{\omega}{\bar{\omega}_0} \right) \quad (8.34)$$

This coincides with the expression for the phase of the single pole, Eq. (8.26). So the right half-plane zero exhibits the magnitude response of the left half-plane zero, but the phase response of the pole. Magnitude and phase asymptotes are summarized in Fig. 8.13.

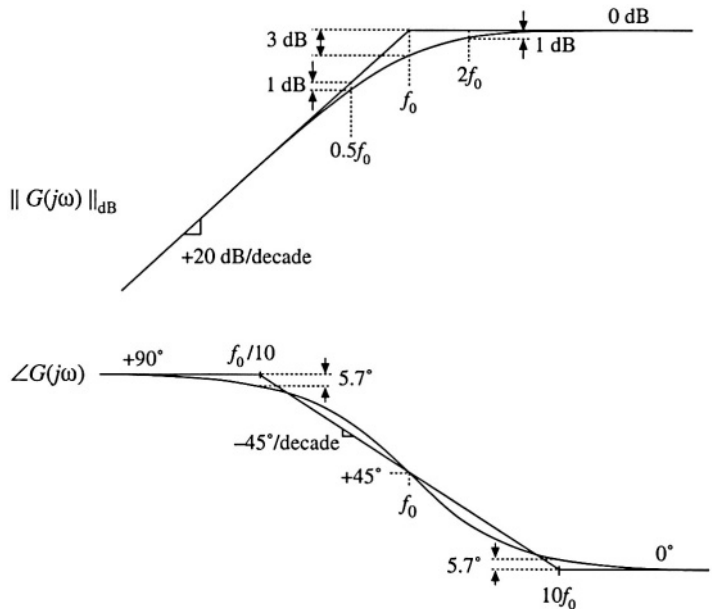


Fig. 8.14 Inversion of the frequency axis: summary of the magnitude and phase Bode plots for the inverted real pole.

8.1.4 Frequency Inversion

Two other forms arise, from inversion of the frequency axis. The inverted pole has the transfer function

$$G(s) = \frac{1}{\left(1 + \frac{\omega_0}{s}\right)} \quad (8.35)$$

As illustrated in Fig. 8.14, the inverted pole has a high-frequency gain of 1, and a low frequency asymptote having a +20 dB/decade slope. This form is useful for describing the gain of high-pass filters, and of other transfer functions where it is desired to emphasize the high frequency gain, with attenuation of low frequencies. Equation (8.35) is equivalent to

$$G(s) = \frac{\left(\frac{s}{\omega_0}\right)}{\left(1 + \frac{s}{\omega_0}\right)} \quad (8.36)$$

However, Eq. (8.35) more directly emphasizes that the high frequency gain is 1.

The inverted zero has the form

$$G(s) = \left(1 + \frac{\omega_0}{s}\right)^{-1} \quad (8.37)$$

As illustrated in Fig. 8.15, the inverted zero has a high-frequency gain asymptote equal to 1, and a low-frequency asymptote having a slope equal to -20 dB/decade. An example of the use of this type of trans-

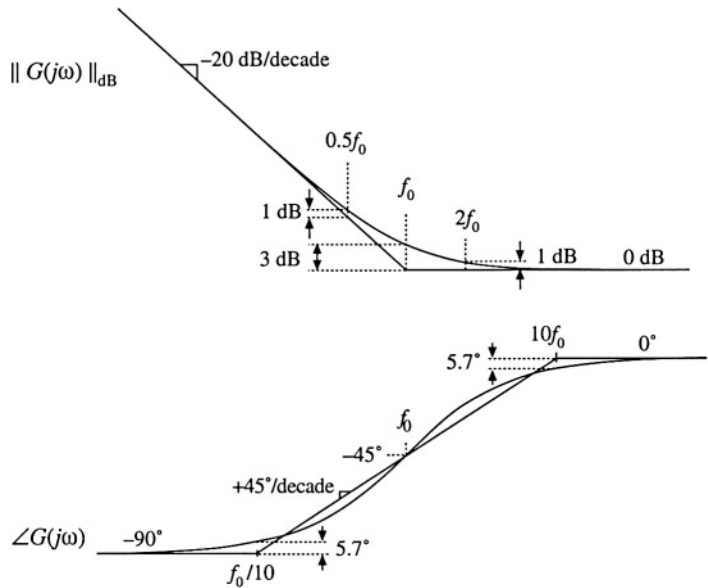


Fig. 8.15 Inversion of the frequency axis: summary of the magnitude and phase Bode plot for the inverted real zero.

fer function is the proportional-plus-integral controller, discussed in connection with feedback loop design in the next chapter. Equation (8.37) is equivalent to

$$G(s) = \frac{\left(1 + \frac{s}{\omega_0}\right)}{\left(\frac{s}{\omega_0}\right)} \quad (8.38)$$

However, Eq. (8.37) is the preferred form when it is desired to emphasize the value of the high-frequency gain asymptote.

The use of frequency inversion is illustrated by example in the next section.

8.1.5 Combinations

The Bode diagram of a transfer function containing several pole, zero, and gain terms, can be constructed by simple addition. At any given frequency, the magnitude (in decibels) of the composite transfer function is equal to the sum of the decibel magnitudes of the individual terms. Likewise, at a given frequency the phase of the composite transfer function is equal to the sum of the phases of the individual terms.

For example, suppose that we have already constructed the Bode diagrams of two complex-valued functions of ω , $G_1(\omega)$ and $G_2(\omega)$. These functions have magnitudes $R_1(\omega)$ and $R_2(\omega)$, and phases $\theta_1(\omega)$ and $\theta_2(\omega)$, respectively. It is desired to construct the Bode diagram of the product $G_3(\omega) = G_1(\omega)G_2(\omega)$. Let $G_3(\omega)$ have magnitude $R_3(\omega)$, and phase $\theta_3(\omega)$. To find this magnitude and phase, we can express $G_1(\omega)$, $G_2(\omega)$, and $G_3(\omega)$ in polar form:

$$\begin{aligned} G_1(\omega) &= R_1(\omega) e^{j\theta_1(\omega)} \\ G_2(\omega) &= R_2(\omega) e^{j\theta_2(\omega)} \\ G_3(\omega) &= R_3(\omega) e^{j\theta_3(\omega)} \end{aligned} \quad (8.39)$$

The product $G_3(\omega)$ can then be expressed as

$$G_3(\omega) = G_1(\omega)G_2(\omega) = R_1(\omega)e^{j\theta_1(\omega)}R_2(\omega)e^{j\theta_2(\omega)} \quad (8.40)$$

Simplification leads to

$$G_3(\omega) = (R_1(\omega)R_2(\omega)) e^{j(\theta_1(\omega) + \theta_2(\omega))} \quad (8.41)$$

Hence, the composite phase is

$$\theta_3(\omega) = \theta_1(\omega) + \theta_2(\omega) \quad (8.42)$$

The total magnitude is

$$R_3(\omega) = R_1(\omega)R_2(\omega) \quad (8.43)$$

When expressed in decibels, Eq. (8.43) becomes

$$|R_3(\omega)|_{dB} = |R_1(\omega)|_{dB} + |R_2(\omega)|_{dB} \quad (8.44)$$

So the composite phase is the sum of the individual phases, and when expressed in decibels, the composite magnitude is the sum of the individual magnitudes. The composite magnitude slope, in dB per decade, is therefore also the sum of the individual slopes in dB per decade.

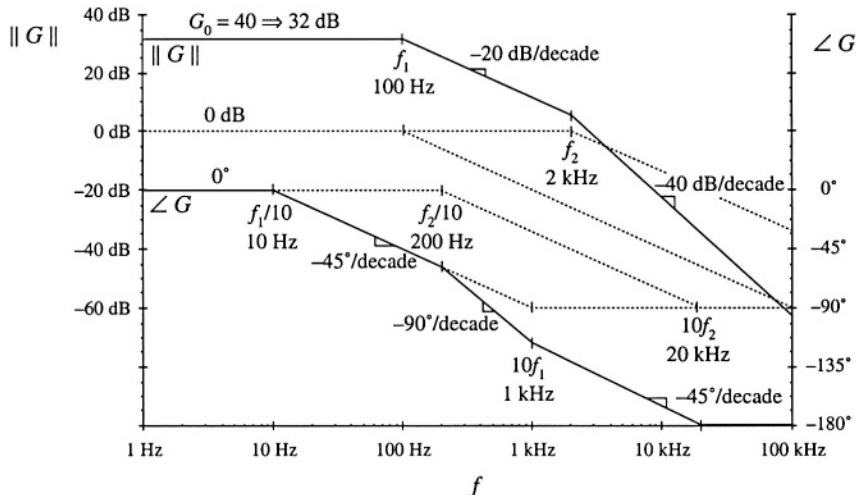


Fig. 8.16 Construction of magnitude and phase asymptotes for the transfer function of Eq.(8.45). Dashed line.

For example, consider construction of the Bode plot of the following transfer function:

$$G(s) = \frac{G_0}{\left(1 + \frac{s}{\omega_1}\right)\left(1 + \frac{s}{\omega_2}\right)} \quad (8.45)$$

where $G_0 = 40 \Rightarrow 32 \text{ dB}$, $f_1 = \omega_1/2\pi = 100 \text{ Hz}$, $f_2 = \omega_2/2\pi = 2 \text{ kHz}$. This transfer function contains three terms: the gain G_0 , and the poles at frequencies f_1 and f_2 . The asymptotes for each of these terms are illustrated in Fig. 8.16. The gain G_0 is a positive real number, and therefore contributes zero phase shift with the gain 32 dB. The poles at 100 Hz and 2 kHz each contribute asymptotes as in Fig. 8.11.

At frequencies less than 100 Hz, the G_0 term contributes a gain magnitude of 32 dB, while the two poles each contribute magnitude asymptotes of 0 dB. So the low-frequency composite magnitude asymptote is $32 \text{ dB} + 0 \text{ dB} + 0 \text{ dB} = 32 \text{ dB}$. For frequencies between 100 Hz and 2 kHz, the G_0 gain again contributes 32 dB, and the pole at 2 kHz continues to contribute a 0 dB magnitude asymptote. However, the pole at 100 Hz now contributes a magnitude asymptote that decreases with a $-20 \text{ dB per decade}$ slope. The composite magnitude asymptote therefore also decreases with a $-20 \text{ dB per decade}$ slope, as illustrated in Fig. 8.16. For frequencies greater than 2 kHz, the poles at 100 Hz and 2 kHz each contribute decreasing asymptotes having slopes of -20 dB/decade . The composite asymptote therefore decreases with a slope of $-20 \text{ dB/decade} - 20 \text{ dB/decade} = -40 \text{ dB/decade}$, as illustrated.

The composite phase asymptote is also constructed in Fig. 8.16. Below 10 Hz, all terms contribute 0° asymptotes. For frequencies between $f_1/10 = 10 \text{ Hz}$, and $f_2/10 = 200 \text{ Hz}$, the pole at f_1 contributes a decreasing phase asymptote having a slope of $-45^\circ/\text{decade}$. Between 200 Hz and $10f_1 = 1 \text{ kHz}$, both poles contribute decreasing asymptotes with $-45^\circ/\text{decade}$ slopes; the composite slope is therefore $-90^\circ/\text{decade}$. Between 1 kHz and $10f_2 = 20 \text{ kHz}$, the pole at f_1 contributes a constant -90° phase asymptote, while the pole at f_2 contributes a decreasing asymptote with $-45^\circ/\text{decade}$ slope. The composite slope is then $-45^\circ/\text{decade}$. For frequencies greater than 20 kHz, both poles contribute constant -90° asymptotes, leading to a composite phase asymptote of -180° .

As a second example, consider the transfer function $A(s)$ represented by the magnitude and phase asymptotes of Fig. 8.17. Let us write the transfer function that corresponds to these asymptotes. The dc asymptote is A_0 . At corner frequency f_1 , the asymptote slope increases from 0 dB/decade to $+20 \text{ dB/decade}$. Hence, there must be a zero at frequency f_1 . At frequency f_2 , the asymptote slope decreases from $+20 \text{ dB/decade}$ to 0 dB/decade. Therefore the transfer function contains a pole at frequency f_2 . So we can express the transfer function as

$$A(s) = A_0 \frac{\left(1 + \frac{s}{\omega_1}\right)}{\left(1 + \frac{s}{\omega_2}\right)} \quad (8.46)$$

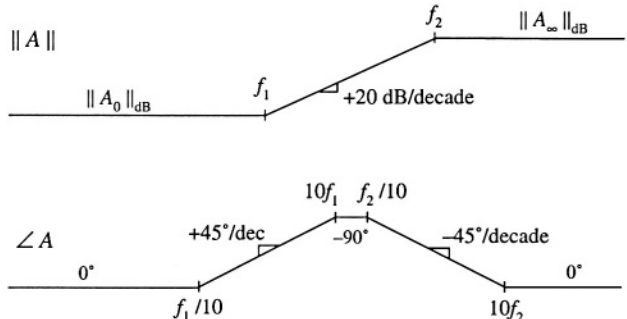


Fig. 8.17 Magnitude and phase asymptotes of example transfer function $A(s)$.

where ω_1 and ω_2 are equal to $2\pi f_1$ and $2\pi f_2$, respectively.

We can use Eq. (8.46) to derive analytical expressions for the asymptotes. For $f < f_1$, and letting $s = j\omega$, we can see that the (s/ω_1) and (s/ω_2) terms each have magnitude less than 1. The asymptote is derived by neglecting these terms. Hence, the low-frequency magnitude asymptote is

$$\left| A_0 \frac{\left(1 + \frac{s}{\omega_1}\right)}{\left(1 + \frac{s}{\omega_2}\right)} \right|_{s=j\omega} = A_0 \frac{1}{1} = A_0 \quad (8.47)$$

For $f_1 < f < f_2$, the numerator term (s/ω_1) has magnitude greater than 1, while the denominator term (s/ω_2) has magnitude less than 1. The asymptote is derived by neglecting the smaller terms:

$$\left| A_0 \frac{\left(j + \frac{s}{\omega_1}\right)}{\left(j + \frac{s}{\omega_2}\right)} \right|_{s=j\omega} = A_0 \frac{\left|\frac{s}{\omega_1}\right|_{s=j\omega}}{1} = A_0 \frac{\omega_1}{\omega_1} = A_0 \frac{f}{f_1} \quad (8.48)$$

This is the expression for the midfrequency magnitude asymptote of $A(s)$. For $f > f_2$, the (s/ω_1) and (s/ω_2) terms each have magnitude greater than 1. The expression for the high-frequency asymptote is therefore:

$$\left| A_0 \frac{\left(j + \frac{s}{\omega_1}\right)}{\left(j + \frac{s}{\omega_2}\right)} \right|_{s=j\omega} = A_0 \frac{\left|\frac{s}{\omega_2}\right|_{s=j\omega}}{\left|\frac{s}{\omega_1}\right|_{s=j\omega}} = A_0 \frac{\omega_2}{\omega_1} = A_0 \frac{f_2}{f_1} \quad (8.49)$$

We can conclude that the high-frequency gain is

$$A_\infty = A_0 \frac{f_2}{f_1} \quad (8.50)$$

Thus, we can derive analytical expressions for the asymptotes.

The transfer function $A(s)$ can also be written in a second form, using inverted poles and zeroes. Suppose that $A(s)$ represents the transfer function of a high-frequency amplifier, whose dc gain is not important. We are then interested in expressing $A(s)$ directly in terms of the high-frequency gain A_∞ . We can view the transfer function as having an inverted pole at frequency f_2 , which introduces attenuation at frequencies less than f_2 . In addition, there is an inverted zero at $f = f_1$. So $A(s)$ could also be written

$$A(s) = A_\infty \frac{\left(1 + \frac{\omega_1}{s}\right)}{\left(1 + \frac{\omega_2}{s}\right)} \quad (8.51)$$

It can be verified that Eqs. (8.51) and (8.46) are equivalent.

8.1.6 Quadratic Pole Response: Resonance

Consider next the transfer function $G(s)$ of the two-pole low-pass filter of Fig. 8.18. The buck converter contains a filter of this type. When manipulated into canonical form, the models of the boost and buck-boost also contain similar filters. One can show that the transfer function of this network is

$$G(s) = \frac{v_2(s)}{v_1(s)} = \frac{1}{1 + s\frac{L}{R} + s^2LC} \quad (8.52)$$

This transfer function contains a second-order denominator polynomial, and is of the form

$$G(s) = \frac{1}{1 + a_1s + a_2s^2} \quad (8.53)$$

with $a_1 = L/R$ and $a_2 = LC$.

To construct the Bode plot of this transfer function, we might try to factor the denominator into its two roots:

$$G(s) = \frac{1}{\left(1 - \frac{s}{s_1}\right)\left(1 - \frac{s}{s_2}\right)} \quad (8.54)$$

Use of the quadratic formula leads to the following expressions for the roots:

$$s_1 = -\frac{a_1}{2a_2} \left[1 - \sqrt{1 - \frac{4a_2}{a_1^2}} \right] \quad (8.55)$$

$$s_2 = -\frac{a_1}{2a_2} \left[1 + \sqrt{1 - \frac{4a_2}{a_1^2}} \right] \quad (8.56)$$

If $4a_2 \leq a_1^2$, then the roots are real. Each real pole then exhibits a Bode diagram as derived in Section 8.1.1, and the composite Bode diagram can be constructed as described in Section 8.1.5 (but a better approach is described in Section 8.1.7).

If $4a_2 > a_1^2$, then the roots (8.55) and (8.56) are complex. In Section 8.1.1, the assumption was made that ω_0 is real; hence, the results of that section cannot be applied to this case. We need to do some additional work, to determine the magnitude and phase for the case when the roots are complex.

The transfer functions of Eqs. (8.52) and (8.53) can be written in the following standard normalized form:

$$G(s) = \frac{1}{1 + 2\zeta \frac{s}{\omega_0} + \left(\frac{s}{\omega_0}\right)^2} \quad (8.57)$$

If the coefficients a_1 and a_2 are real and positive, then the parameters ζ and ω_0 are also real and positive. The parameter ω_0 is again the angular corner frequency, and we can define $f_0 = \omega_0/2\pi$. The parameter ζ is

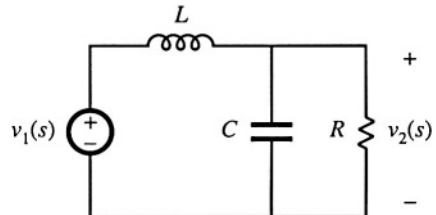


Fig. 8.18 Two-pole low-pass filter example.

called the *damping factor*: ζ controls the shape of the transfer function in the vicinity of $f = f_0$. An alternative standard normalized form is

$$G(s) = \frac{1}{1 + \frac{s}{Q\omega_0} + \left(\frac{s}{\omega_0}\right)^2} \quad (8.58)$$

where

$$Q = \frac{1}{2\zeta} \quad (8.59)$$

The parameter Q is called the *quality factor* of the circuit, and is a measure of the dissipation in the system. A more general definition of Q , for sinusoidal excitation of a passive element or network, is

$$Q = 2\pi \frac{(\text{peak stored energy})}{(\text{energy dissipated per cycle})} \quad (8.60)$$

For a second-order passive system, Eqs. (8.59) and (8.60) are equivalent. We will see that the Q -factor has a very simple interpretation in the magnitude Bode diagrams of second-order transfer functions.

Analytical expressions for the parameters Q and ω_0 can be found by equating like powers of s in the original transfer function, Eq. (8.52), and in the normalized form, Eq. (8.58). The result is

$$\begin{aligned} f_0 &= \frac{\omega_0}{2\pi} = \frac{1}{2\pi\sqrt{LC}} \\ Q &= R\sqrt{\frac{C}{L}} \end{aligned} \quad (8.61)$$

The roots s_1 and s_2 of Eqs. (8.55) and (8.56) are real when $Q \leq 0.5$, and are complex when $Q > 0.5$.

The magnitude of G is

$$\|G(j\omega)\| = \sqrt{\left(1 - \left(\frac{\omega}{\omega_0}\right)^2\right)^2 + \frac{1}{Q^2} \left(\frac{\omega}{\omega_0}\right)^2} \quad (8.62)$$

Asymptotes of $\|G\|$ are illustrated in Fig. 8.19. At low frequencies, $(\omega/\omega_0) \ll 1$, and hence

$$\|G\| \rightarrow 1 \quad \text{for } \omega \ll \omega_0 \quad (8.63)$$

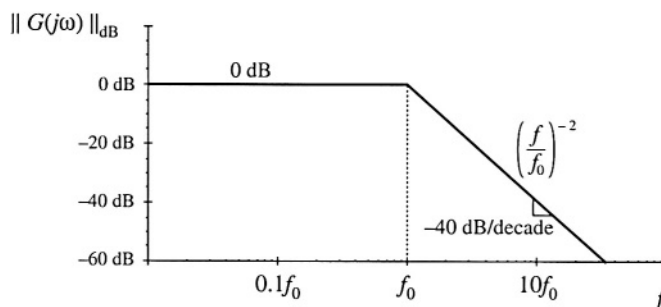


Fig. 8.19 Magnitude asymptotes for the two-pole transfer function.

At high frequencies where $(\omega/\omega_0) \gg 1$, the $(\omega/\omega_0)^4$ term dominates the expression inside the radical of Eq. (8.62). Hence, the high-frequency asymptote is

$$\|G\| \rightarrow \left(\frac{f}{f_0}\right)^{-2} \quad \text{for } \omega \gg \omega_0 \quad (8.64)$$

This expression coincides with Eq. (8.5), with $n = -2$. Therefore, the high-frequency asymptote has slope -40 dB/decade . The asymptotes intersect at $f = f_0$, and are independent of Q .

The parameter Q affects the deviation of the actual curve from the asymptotes, in the neighborhood of the corner frequency f_0 . The exact magnitude at $f = f_0$ is found by substitution of $\omega = \omega_0$ into Eq. (8.62):

$$\|G(j\omega_0)\| = Q \quad (8.65)$$

So the exact transfer function has magnitude Q at the corner frequency f_0 . In decibels, Eq. (8.65) is

$$\|G(j\omega_0)\|_{\text{dB}} = |Q|_{\text{dB}} \quad (8.66)$$

So if, for example, $Q = 2 \Rightarrow 6 \text{ dB}$, then the actual curve deviates from the asymptotes by 6 dB at the corner frequency $f = f_0$. Salient features of the magnitude Bode plot of the second-order transfer function are summarized in Fig. 8.20.

The phase of G is

$$\angle G(j\omega) = -\tan^{-1} \left[\frac{\frac{1}{Q} \left(\frac{\omega}{\omega_0} \right)}{1 - \left(\frac{\omega}{\omega_0} \right)^2} \right] \quad (8.67)$$

The phase tends to 0° at low frequency, and to -180° at high frequency. At $f = f_0$, the phase is -90° . As illustrated in Fig. 8.21, increasing the value of Q causes a sharper phase change between the 0° and -180° asymptotes. We again need a midfrequency asymptote, to approximate the phase transition in the

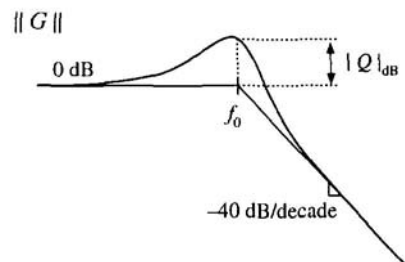


Fig. 8.20 Important features of the magnitude Bode plot, for the two-pole transfer function.

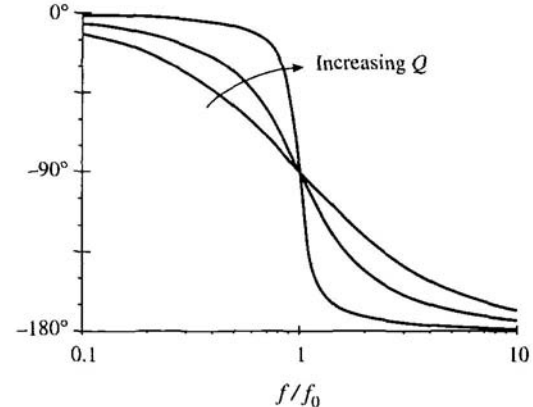


Fig. 8.21 Phase plot, second-order poles. $\angle G$ Increasing Q causes a sharper phase change.

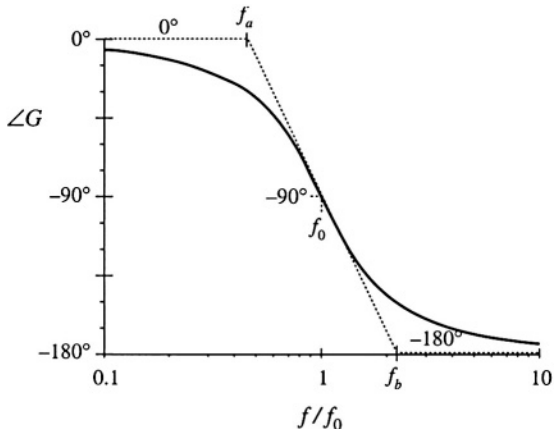


Fig. 8.22 One choice for the midfrequency phase asymptote of the two-pole response, which correctly predicts the actual slope at $f = f_0$.

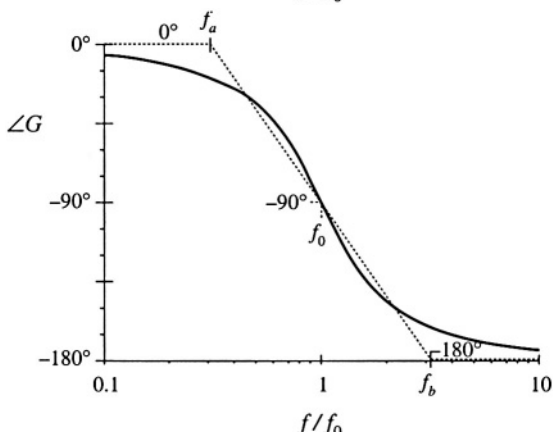


Fig. 8.23 A simpler choice for the midfrequency phase asymptote, which better approximates the curve over the entire frequency range and is consistent with the asymptote used for real poles.

vicinity of the corner frequency f_0 , as illustrated in Fig. 8.22. As in the case of the real single pole, we could choose the slope of this asymptote to be identical to the slope of the actual curve at $f = f_0$. It can be shown that this choice leads to the following asymptote break frequencies:

$$\begin{aligned} f_a &= \left(e^{\pi/2}\right)^{-\frac{1}{2Q}} f_0 \\ f_b &= \left(e^{\pi/2}\right)^{\frac{1}{2Q}} f_0 \end{aligned} \quad (8.68)$$

A better choice, which is consistent with the approximation (8.28) used for the real single pole, is

$$\begin{aligned} f_a &= 10^{-1/2Q} f_0 \\ f_b &= 10^{1/2Q} f_0 \end{aligned} \quad (8.69)$$

With this choice, the midfrequency asymptote has slope $-180Q$ degrees per decade. The phase asymptotes are summarized in Fig. 8.23. With $Q = 0.5$, the phase changes from 0° to -180° over a frequency span of approximately two decades, centered at the corner frequency f_0 . Increasing the Q causes this frequency span to decrease rapidly.

Second-order response magnitude and phase curves are plotted in Figs. 8.24 and 8.25.

Fig. 8.24 Exact magnitude curves, two-pole response, for several values of Q .

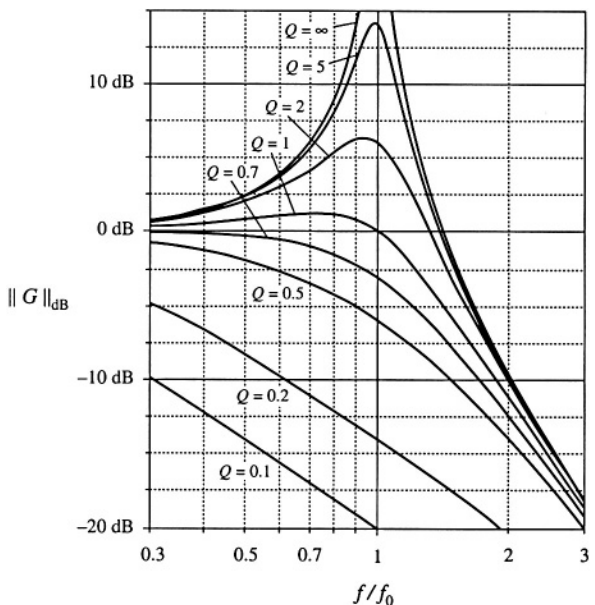
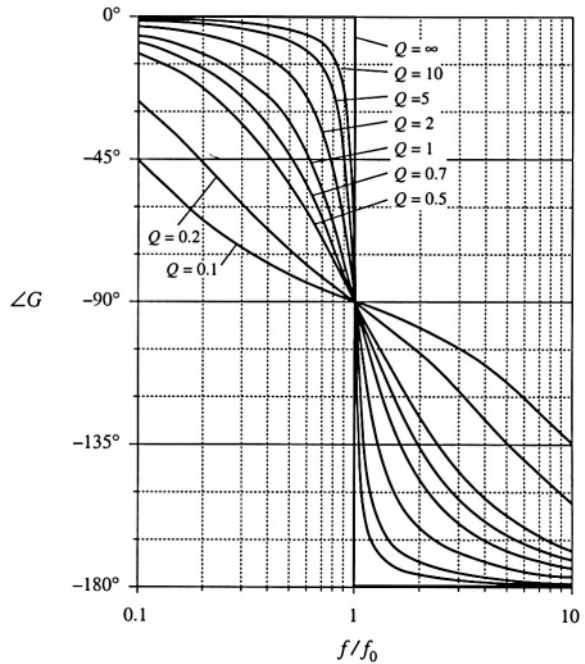


Fig. 8.25 Exact phase curves, two-pole response, for several values of Q .



8.1.7 The Low-Q Approximation

As mentioned in Section 8.1.6, when the roots of second-order denominator polynomial of Eq. (8.53) are real, then we can factor the denominator, and construct the Bode diagram using the asymptotes for real poles. We would then use the following normalized form:

$$G(s) = \frac{1}{\left(1 + \frac{s}{\omega_1}\right)\left(1 + \frac{s}{\omega_2}\right)} \quad (8.70)$$

This is a particularly desirable approach when the corner frequencies ω_1 and ω_2 are well separated in value.

The difficulty in this procedure lies in the complexity of the quadratic formula used to find the corner frequencies. Expressing the corner frequencies ω_1 and ω_2 in terms of the circuit elements R , L , C , etc., invariably leads to complicated and unilluminating expressions, especially when the circuit contains many elements. Even in the case of the simple circuit of Fig. 8.18, whose transfer function is given by Eq. (8.52), the conventional quadratic formula leads to the following complicated formula for the corner frequencies:

$$\omega_1, \omega_2 = \frac{\frac{L}{R} \pm \sqrt{\left(\frac{L}{R}\right)^2 - 4LC}}{2LC} \quad (8.71)$$

This equation yields essentially no insight regarding how the corner frequencies depend on the element values. For example, it can be shown that when the corner frequencies are well separated in value, they can be expressed with high accuracy by the much simpler relations

$$\omega_1 \approx \frac{R}{L}, \quad \omega_2 \approx \frac{1}{RC} \quad (8.72)$$

In this case, ω_1 is essentially independent of the value of C , and ω_2 is essentially independent of L , yet Eq. (8.71) apparently predicts that both corner frequencies are dependent on all element values. The simple expressions of Eq. (8.72) are far preferable to Eq. (8.71), and can be easily derived using the low- Q approximation [2].

Let us assume that the transfer function has been expressed in the standard normalized form of Eq. (8.58), reproduced below:

$$G(s) = \frac{1}{1 + \frac{s}{Q\omega_0} + \left(\frac{s}{\omega_0}\right)^2} \quad (8.73)$$

For $Q \leq 0.5$, let us use the quadratic formula to write the real roots of the denominator polynomial of Eq. (8.73) as

$$\omega_1 = \frac{\omega_0}{Q} \frac{1 - \sqrt{1 - 4Q^2}}{2} \quad (8.74)$$

$$\omega_2 = \frac{\omega_0}{Q} \frac{1 + \sqrt{1 - 4Q^2}}{2} \quad (8.75)$$

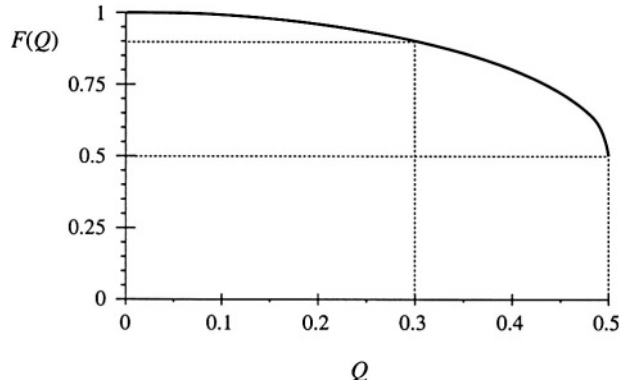


Fig. 8.26 $F(Q)$ vs. Q , as given by Eq. (8.77). The approximation $F(Q) \approx 1$ is within 10% of the exact value for $Q < 3$.

The corner frequency ω_2 can be expressed

$$\omega_2 = \frac{\omega_0}{Q} F(Q) \quad (8.76)$$

where $F(Q)$ is defined as [2]:

$$F(Q) = \frac{1}{2} \left(1 + \sqrt{1 - 4Q^2} \right) \quad (8.77)$$

Note that, when $Q \ll 0.5$, then $4Q^2 \ll 1$ and $F(Q)$ is approximately equal to 1. We then obtain

$$\omega_2 \approx \frac{\omega_0}{Q} \quad \text{for } Q \ll \frac{1}{2} \quad (8.78)$$

The function $F(Q)$ is plotted in Fig. 8.26. It can be seen that $F(Q)$ approaches 1 very rapidly as Q decreases below 0.5.

To derive a similar approximation for ω_1 , we can multiply and divide Eq. (8.74) by $F(Q)$, Eq. (8.77). Upon simplification of the numerator, we obtain

$$\omega_1 = \frac{Q\omega_0}{F(Q)} \quad (8.79)$$

Again, $F(Q)$ tends to 1 for small Q . Hence, ω_1 can be approximated as

$$\omega_1 \approx Q\omega_0 \quad \text{for } Q \ll \frac{1}{2} \quad (8.80)$$

Magnitude asymptotes for the low- Q case are summarized in Fig. 8.27. For $Q < 0.5$, the two poles at ω_0 split into real poles. One real pole occurs at corner frequency $\omega_1 < \omega_0$, while the other occurs at corner frequency $\omega_2 > \omega_0$. The corner frequencies are easily approximated, using Eqs. (8.78) and (8.80).

For the filter circuit of Fig. 8.18, the parameters Q and ω_0 are given by Eq. (8.61). For the case when $Q \ll 0.5$, we can derive the following analytical expressions for the corner frequencies, using Eqs. (8.78) and (8.80):

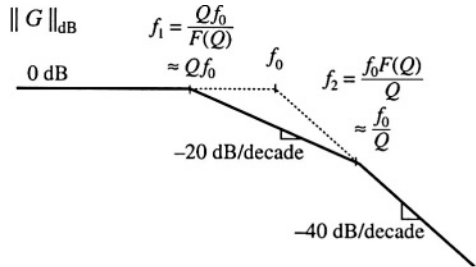


Fig. 8.27 Magnitude asymptotes predicted by the low- Q approximation. Real poles occur at frequencies Qf_0 and f_0/Q .

$$\begin{aligned}\omega_1 &\approx Q\omega_0 = R \sqrt{\frac{C}{L}} \frac{1}{\sqrt{LC}} = \frac{R}{L} \\ \omega_2 &\approx \frac{\omega_0}{Q} = \frac{1}{\sqrt{LC}} \frac{1}{R \sqrt{\frac{C}{L}}} = \frac{1}{RC}\end{aligned}\quad (8.81)$$

So the low- Q approximation allows us to derive simple design-oriented analytical expressions for the corner frequencies.

8.1.8 Approximate Roots of an Arbitrary-Degree Polynomial

The low- Q approximation can be generalized, to find approximate analytical expressions for the roots of the n^{th} -order polynomial

$$P(s) = 1 + a_1 s + a_2 s^2 + \cdots + a_n s^n \quad (8.82)$$

It is desired to factor the polynomial $P(s)$ into the form

$$P(s) = (1 + \tau_1 s)(1 + \tau_2 s) \cdots (1 + \tau_n s) \quad (8.83)$$

In a real circuit, the coefficients a_1, \dots, a_n are real, while the time constants τ_1, \dots, τ_n may be either real or complex. Very often, some or all of the time constants are well separated in value, and depend in a very simple way on the circuit element values. In such cases, simple approximate analytical expressions for the time constants can be derived.

The time constants τ_1, \dots, τ_n can be related to the original coefficients a_1, \dots, a_n by multiplying out Eq. (8.83). The result is

$$\begin{aligned}a_1 &= \tau_1 + \tau_2 + \cdots + \tau_n \\ a_2 &= \tau_1(\tau_2 + \cdots + \tau_n) + \tau_2(\tau_3 + \cdots + \tau_n) + \cdots \\ a_3 &= \tau_1\tau_2(\tau_3 + \cdots + \tau_n) + \tau_2\tau_3(\tau_4 + \cdots + \tau_n) + \cdots \\ &\vdots \\ a_n &= \tau_1\tau_2\tau_3 \cdots \tau_n\end{aligned}\quad (8.84)$$

General solution of this system of equations amounts to exact factoring of the arbitrary degree polynomial, a hopeless task. Nonetheless, Eq. (8.84) does suggest a way to approximate the roots.

Suppose that all of the time constants τ_1, \dots, τ_n are real and well separated in value. We can further assume, without loss of generality, that the time constants are arranged in decreasing order of magni-

tude:

$$|\tau_1| \gg |\tau_2| \gg \dots \gg |\tau_n| \quad (8.85)$$

When the inequalities of Eq. (8.85) are satisfied, then the expressions for a_1, \dots, a_n of Eq. (8.84) are each dominated by their first terms:

$$\begin{aligned} a_1 &\approx \tau_1 \\ a_2 &\approx \tau_1 \tau_2 \\ a_3 &\approx \tau_1 \tau_2 \tau_3 \\ &\vdots \\ a_n &= \tau_1 \tau_2 \tau_3 \cdots \tau_n \end{aligned} \quad (8.86)$$

These expressions can now be solved for the time constants, with the result

$$\begin{aligned} \tau_1 &\approx a_1 \\ \tau_2 &\approx \frac{a_2}{a_1} \\ \tau_3 &\approx \frac{a_3}{a_2} \\ &\vdots \\ \tau_n &\approx \frac{a_n}{a_{n-1}} \end{aligned} \quad (8.87)$$

Hence, if

$$|a_1| \gg \left| \frac{a_2}{a_1} \right| \gg \left| \frac{a_3}{a_2} \right| \gg \dots \gg \left| \frac{a_n}{a_{n-1}} \right| \quad (8.88)$$

then the polynomial $P(s)$ given by Eq. (8.82) has the approximate factorization

$$P(s) \approx \left(1 + a_1 s\right) \left(1 + \frac{a_2}{a_1} s\right) \left(1 + \frac{a_3}{a_2} s\right) \cdots \left(1 + \frac{a_n}{a_{n-1}} s\right) \quad (8.89)$$

Note that if the original coefficients in Eq. (8.82) are simple functions of the circuit elements, then the approximate roots given by Eq. (8.89) are similar simple functions of the circuit elements. So approximate analytical expressions for the roots can be obtained. Numerical values are substituted into Eq. (8.88) to justify the approximation.

In the case where two of the roots are not well separated, then one of the inequalities of Eq. (8.88) is violated. We can then leave the corresponding terms in quadratic form. For example, suppose that inequality k is not satisfied:

$$|a_1| \gg \left| \frac{a_2}{a_1} \right| \gg \dots \gg \left| \frac{a_k}{a_{k-1}} \right| \gg \left| \frac{a_{k+1}}{a_k} \right| \gg \dots \gg \left| \frac{a_n}{a_{n-1}} \right| \quad (8.90)$$

Then an approximate factorization is

$$(8.91) \quad \|G\|_{dB} = 20 \log_{10}(\|G\|)$$

The conditions for accuracy of this approximation are

$$|a_1| \gg \left| \frac{a_2}{a_1} \right| \gg \dots \gg \left| \frac{a_k}{a_{k-1}} \right| \gg \left| \frac{a_{k-2} a_{k+1}}{a_{k-1}^2} \right| \gg \left| \frac{a_{k+2}}{a_{k+1}} \right| \gg \dots \gg \left| \frac{a_n}{a_{n-1}} \right| \quad (8.92)$$

Complex conjugate roots can be approximated in this manner.

When the first inequality of Eq. (8.88) is violated, that is,

$$|a_1| \not\gg \left| \frac{a_2}{a_1} \right| \gg \left| \frac{a_3}{a_2} \right| \gg \dots \gg \left| \frac{a_n}{a_{n-1}} \right| \quad (8.93)$$

then the first two roots should be left in quadratic form

$$P(s) \approx \left(1 + a_1 s + a_2 s^2 \right) \left(1 + \frac{a_3}{a_2} s \right) \dots \left(1 + \frac{a_n}{a_{n-1}} s \right) \quad (8.94)$$

This approximation is justified provided that

$$\left| \frac{a_2^2}{a_3} \right| \gg |a_1| \gg \left| \frac{a_3}{a_2} \right| \gg \left| \frac{a_4}{a_3} \right| \gg \dots \gg \left| \frac{a_n}{a_{n-1}} \right| \quad (8.95)$$

If none of the above approximations is justified, then there are three or more roots that are close in magnitude. One must then resort to cubic or higher-order forms.

As an example, consider the damped EMI filter illustrated in Fig. 8.28. Filters such as this are typically placed at the power input of a converter, to attenuate the switching harmonics present in the converter input current. By circuit analysis, one can show that this filter exhibits the following transfer function:

$$G(s) = \frac{i_g(s)}{i_c(s)} = \frac{1 + s \frac{L_1 + L_2}{R}}{1 + s \frac{L_1 + L_2}{R} + s^2 L_1 C + s^3 \frac{L_1 L_2 C}{R}} \quad (8.96)$$

This transfer function contains a third-order denominator, with the following coefficients:

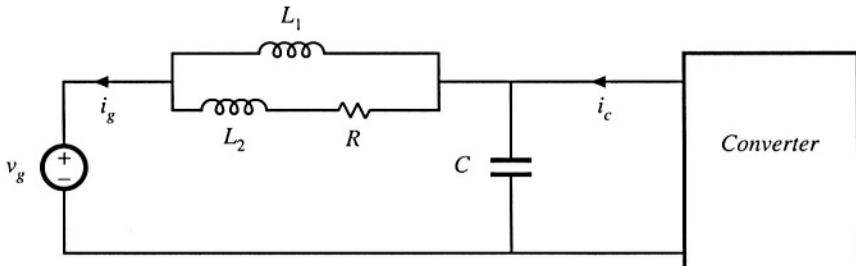


Fig. 8.28 Input EMI filter example.

$$\begin{aligned} a_1 &= \frac{L_1 + L_2}{R} \\ a_2 &= L_1 C \\ a_3 &= \frac{L_1 L_2 C}{R} \end{aligned} \tag{8.97}$$

It is desired to factor the denominator, to obtain analytical expressions for the poles. The correct way to do this depends on the numerical values of R , L_1 , L_2 , and C . When the roots are real and well separated, then Eq. (8.89) predicts that the denominator can be factored as follows:

$$\left(1 + s \frac{L_1 + L_2}{R}\right) \left(1 + sRC \frac{L_1}{L_1 + L_2}\right) \left(1 + s \frac{L_2}{R}\right) \tag{8.98}$$

According to Eq. (8.88), this approximation is justified provided that

$$\frac{L_1 + L_2}{R} \gg RC \frac{L_1}{L_1 + L_2} \gg \frac{L_2}{R} \tag{8.99}$$

These inequalities cannot be satisfied unless $L_1 \gg L_2$. When $L_1 \gg L_2$, then Eq. (8.99) can be further simplified to

$$\frac{L_1}{R} \gg RC \gg \frac{L_2}{R} \tag{8.100}$$

The approximate factorization, Eq. (8.98), can then be further simplified to

$$\left(1 + s \frac{L_1}{R}\right) \left(1 + sRC\right) \left(1 + s \frac{L_2}{R}\right) \tag{8.101}$$

Thus, in this case the transfer function contains three well separated real poles. Equations (8.98) and (8.101) represent approximate analytical factorizations of the denominator of Eq. (8.96). Although numerical values must be substituted into Eqs. (8.99) or (8.100) to justify the approximation, we can nonetheless express Eqs. (8.98) and (8.101) as analytical functions of L_1 , L_2 , R , and C . Equations (8.98) and (8.101) are design-oriented, because they yield insight into how the element values can be chosen such that given specified pole frequencies are obtained.

When the second inequality of Eq. (8.99) is violated,

$$\frac{L_1 + L_2}{R} \gg RC \frac{L_1}{L_1 + L_2} \not\gg \frac{L_2}{R} \tag{8.102}$$

then the second and third roots should be left in quadratic form:

$$\left(1 + s \frac{L_1 + L_2}{R}\right) \left(1 + sRC \frac{L_1}{L_1 + L_2} + s^2 L_1 || L_2 C\right) \tag{8.103}$$

This expression follows from Eq. (8.91), with $k = 2$. Equation (8.92) predicts that this approximation is justified provided that

$$\frac{L_1 + L_2}{R} \gg RC \frac{L_1}{L_1 + L_2} \gg \frac{L_1 \| L_2}{L_1 + L_2} RC \quad (8.104)$$

In application of Eq. (8.92), we take a_0 to be equal to 1. The inequalities of Eq. (8.104) can be simplified to obtain

$$L_1 \gg L_2, \quad \text{and} \quad \frac{L_1}{R} \gg RC \quad (8.105)$$

Note that it is no longer required that $RC \gg L_2/R$. Equation (8.105) implies that factorization (8.103) can be further simplified to

$$\left(1 + s \frac{L_1}{R}\right) \left(1 + sRC + s^2 L_2 C\right) \quad (8.106)$$

Thus, for this case, the transfer function contains a low-frequency pole that is well separated from a high-frequency quadratic pole pair. Again, the factored result (8.106) is expressed as an analytical function of the element values, and consequently is design-oriented.

In the case where the first inequality of Eq. (8.99) is violated:

$$\frac{L_1 + L_2}{R} \not\gg RC \frac{L_1}{L_1 + L_2} \not\gg \frac{L_2}{R} \quad (8.107)$$

then the first and second roots should be left in quadratic form:

$$\left(1 + s \frac{L_1 + L_2}{R} + s^2 L_1 C\right) \left(1 + s \frac{L_2}{R}\right) \quad (8.108)$$

This expression follows directly from Eq. (8.94). Equation (8.95) predicts that this approximation is justified provided that

$$\frac{L_1 RC}{L_2} \gg \frac{L_1 + L_2}{R} \gg \frac{L_2}{R} \quad (8.109)$$

that is,

$$L_1 \gg L_2, \quad \text{and} \quad RC \gg \frac{L_2}{R} \quad (8.110)$$

For this case, the transfer function contains a low-frequency quadratic pole pair that is well separated from a high-frequency real pole. If none of the above approximations are justified, then all three of the roots are similar in magnitude. We must then find other means of dealing with the original cubic polynomial. Design of input filters, including the filter of Fig. 8.28, is covered in Chapter 10.

8.2 ANALYSIS OF CONVERTER TRANSFER FUNCTIONS

Let us next derive analytical expressions for the poles, zeroes, and asymptote gains in the transfer functions of the basic converters.

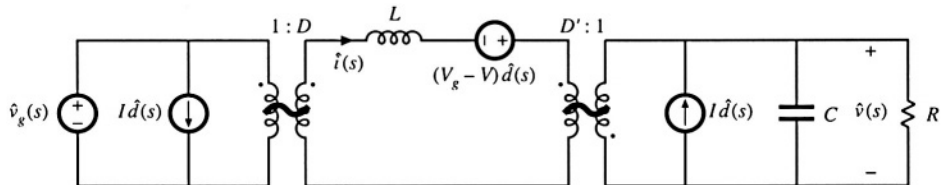


Fig. 8.29 Buck-boost converter equivalent circuit derived in Section 7.2.

8.2.1 Example: Transfer Functions of the Buck-Boost Converter

The small-signal equivalent circuit model of the buck-boost converter is derived in Section 7.2, with the result [Fig. 7.16(b)] repeated in Fig. 8.29. Let us derive and plot the control-to-output and line-to-output transfer functions for this circuit.

The converter contains two independent ac inputs: the control input $\hat{d}(s)$ and the line input $\hat{v}_g(s)$. The ac output voltage variations $\hat{v}(s)$ can be expressed as the superposition of terms arising from these two inputs:

$$\hat{v}(s) = G_{vd}(s)\hat{d}(s) + G_{vg}(s)\hat{v}_g(s) \quad (8.111)$$

Hence, the transfer functions $G_{vd}(s)$ and $G_{vg}(s)$ can be defined as

$$G_{vd}(s) = \left. \frac{\hat{v}(s)}{\hat{d}(s)} \right|_{\hat{v}_g(s)=0} \quad \text{and} \quad G_{vg}(s) = \left. \frac{\hat{v}(s)}{\hat{v}_g(s)} \right|_{\hat{d}(s)=0} \quad (8.112)$$

To find the line-to-output transfer function $G_{vg}(s)$, we set the \hat{d} sources to zero as in Fig. 8.30(a). We can then push the $v_g(s)$ source and the inductor through the transformers, to obtain the circuit of Fig. 8.30(b). The transfer function $G_{vg}(s)$ is found using the voltage divider formula:

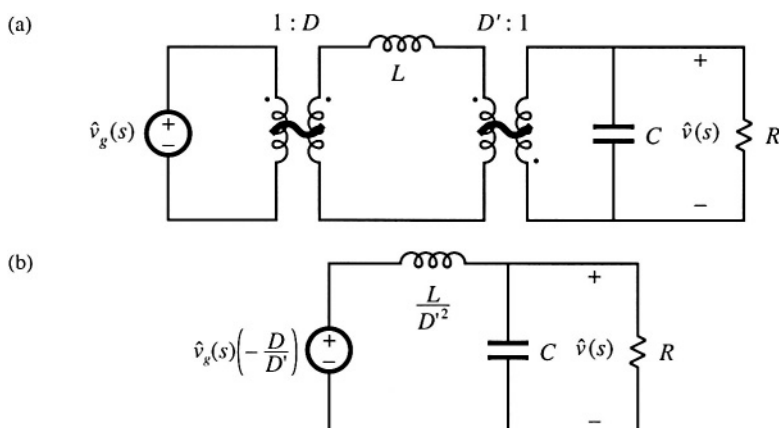


Fig. 8.30 Manipulation of buck-boost equivalent circuit to find the line-to-output transfer function $G_{vg}(s)$: (a) set \hat{d} sources to zero; (b) push inductor and \hat{v}_g source through transformers.

$$G_{vg}(s) = \left. \frac{\hat{v}(s)}{\hat{v}_g(s)} \right|_{d(s)=0} = -\frac{D}{D'} \frac{\left(R \parallel \frac{1}{sC} \right)}{\frac{sL}{D'^2} + \left(R \parallel \frac{1}{sC} \right)} \quad (8.113)$$

We next expand the parallel combination, and express as a rational fraction:

$$\begin{aligned} G_{vg}(s) &= \left(-\frac{D}{D'} \right) \frac{\left(\frac{R}{1+sRC} \right)}{\frac{sL}{D'^2} + \left(\frac{R}{1+sRC} \right)} \\ &= \left(-\frac{D}{D'} \right) \frac{R}{R + \frac{sL}{D'^2} + \frac{s^2RLC}{D'^2}} \end{aligned} \quad (8.114)$$

We aren't done yet—the next step is to manipulate the expression into normalized form, such that the coefficients of s^0 in the numerator and denominator polynomials are equal to one. This can be accomplished by dividing the numerator and denominator by R :

$$G_{vg}(s) = \left. \frac{\hat{v}(s)}{\hat{v}_g(s)} \right|_{d(s)=0} = \left(-\frac{D}{D'} \right) \frac{1}{1 + s \frac{L}{D'^2 R} + s^2 \frac{LC}{D'^2}} \quad (8.115)$$

Thus, the line-to-output transfer function contains a dc gain G_{g0} and a quadratic pole pair:

$$G_{vg}(s) = G_{g0} \frac{1}{1 + \frac{s}{Q\omega_0} + \left(\frac{s}{\omega_0} \right)^2} \quad (8.116)$$

Analytical expressions for the salient features of the line-to-output transfer function are found by equating like terms in Eqs. (8.115) and (8.116). The dc gain is

$$G_{g0} = -\frac{D}{D'} \quad (8.117)$$

By equating the coefficients of s^2 in the denominators of Eqs. (8.115) and (8.116), we obtain

$$\frac{1}{\omega_0^2} = \frac{LC}{D'^2} \quad (8.118)$$

Hence, the angular corner frequency is

$$\omega_0 = \frac{D'}{\sqrt{LC}} \quad (8.119)$$

By equating coefficients of s in the denominators of Eqs. (8.115) and (8.116), we obtain

$$\frac{1}{Q\omega_0} = \frac{L}{D'^2 R} \quad (8.120)$$

Elimination of ω_0 using Eq. (8.119) and solution for Q leads to

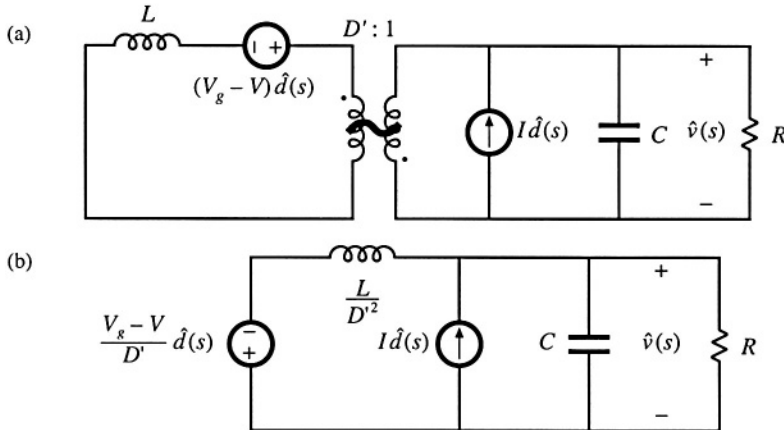


Fig. 8.31 Manipulation of buck-boost equivalent circuit to find the control-to-output transfer function $G_{vd}(s)$: (a) set \hat{v}_g source to zero; (b) push inductor and voltage source through transformer.

$$Q = D'R \sqrt{\frac{C}{L}} \quad (8.121)$$

Equations (8.117), (8.119), and (8.121) are the desired results in the analysis of the line-to-output transfer function. These expressions are useful not only in analysis situations, where it is desired to find numerical values of the salient features G_{gd} , ω_0 , and Q , but also in design situations, where it is desired to select numerical values for R , L , and C such that given values of the salient features are obtained.

Derivation of the control-to-output transfer function $G_{vd}(s)$ is complicated by the presence in Fig. 8.29 of three generators that depend on $\hat{d}(s)$. One good way to find $G_{vd}(s)$ is to manipulate the circuit model as in the derivation of the canonical model, Fig. 7.60. Another approach, used here, employs the principle of superposition. First, we set the \hat{v}_g source to zero. This shorts the input to the $1:D$ transformer, and we are left with the circuit illustrated in Fig. 8.31(a). Next, we push the inductor and \hat{d} voltage source through the $D':1$ transformer, as in Fig. 8.31(b).

Figure 8.31(b) contains a \hat{d} -dependent voltage source and a \hat{d} -dependent current source. The transfer function $G_{vd}(s)$ can therefore be expressed as a superposition of terms arising from these two sources. When the current source is set to zero (i.e., open-circuited), the circuit of Fig. 8.32(a) is obtained. The output $\hat{v}(s)$ can then be expressed as

$$\frac{\hat{v}(s)}{\hat{d}(s)} = \left(-\frac{V_g - V}{D'} \right) \frac{\left(R \parallel \frac{1}{sC} \right)}{\frac{sL}{D'^2} + \left(R \parallel \frac{1}{sC} \right)} \quad (8.122)$$

When the voltage source is set to zero (i.e., short-circuited), Fig. 8.31(b) reduces to the circuit illustrated in Fig. 8.32(b). The output $\hat{v}(s)$ can then be expressed as

$$\frac{\hat{v}(s)}{\hat{d}(s)} = I \left(\frac{sL}{D'^2} \parallel R \parallel \frac{1}{sC} \right) \quad (8.123)$$

The transfer function $G_{vd}(s)$ is the sum of Eqs. (8.122) and (8.123):

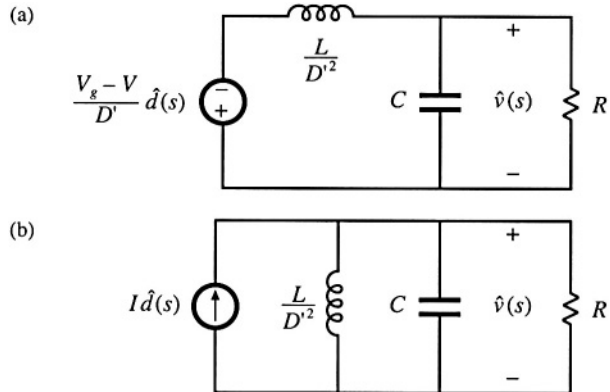


Fig. 8.32 Solution of the model of Fig. 8.32(b) by superposition: (a) current source set to zero; (b) voltage source set to zero.

$$G_{vd}(s) = \left(-\frac{V_g - V}{D'} \right) \frac{\left(R \parallel \frac{1}{sC} \right)}{\frac{sL}{D'^2} + \left(R \parallel \frac{1}{sC} \right)} + I \left(\frac{sL}{D'^2} \parallel R \parallel \frac{1}{sC} \right) \quad (8.124)$$

By algebraic manipulation, one can reduce this expression to

$$G_{vd}(s) = \frac{\hat{v}_d(s)}{\hat{d}(s)} \Big|_{\hat{v}_g(s)=0} = \left(-\frac{V_g - V}{D'} \right) \frac{\left(1 - s \frac{LI}{D'(V_g - V)} \right)}{\left(1 + s \frac{L}{D'^2 R} + s^2 \frac{LC}{D'^2} \right)} \quad (8.125)$$

This equation is of the form

$$G_{vd}(s) = G_{d0} \frac{\left(1 - \frac{s}{\omega_z} \right)}{\left(1 + \frac{s}{Q\omega_0} + \left(\frac{s}{\omega_0} \right)^2 \right)} \quad (8.126)$$

The denominators of Eq. (8.125) and (8.115) are identical, and hence $G_{vd}(s)$ and $G_{vg}(s)$ share the same ω_0 and Q , given by Eqs. (8.119) and (8.121). The dc gain is

$$G_{d0} = -\frac{V_g - V}{D'} = -\frac{V_g}{D'^2} = \frac{V}{DD'} \quad (8.127)$$

The angular frequency of the zero is found by equating coefficients of s in the numerators of Eqs. (8.125) and (8.126). One obtains

$$\omega_z = \frac{D'(V_g - V)}{LI} = \frac{D'^2 R}{DL} \quad (\text{RHP}) \quad (8.128)$$

This zero lies in the right half-plane. Equations (8.127) and (8.128) have been simplified by use of the dc relationships

$$\begin{aligned} V &= -\frac{D}{D'} V_g \\ I &= -\frac{V}{D'R} \end{aligned} \quad (8.129)$$

Equations (8.119), (8.121), (8.127), and (8.128) constitute the results of the analysis of the control-to-output transfer function: analytical expressions for the salient features ω_0 , Q , G_{d0} , and ω_z . These expressions can be used to choose the element values such that given desired values of the salient features are obtained.

Having found analytical expressions for the salient features of the transfer functions, we can now plug in numerical values and construct the Bode plot. Suppose that we are given the following values:

$$\begin{aligned} D &= 0.6 \\ R &= 10 \Omega \\ V_g &= 30 \text{ V} \\ L &= 160 \mu\text{H} \\ C &= 160 \mu\text{F} \end{aligned} \quad (8.130)$$

We can evaluate Eqs. (8.117), (8.119), (8.121), (8.127), and (8.128), to determine numerical values of the salient features of the transfer functions. The results are:

$$\begin{aligned} |G_{g0}| &= \frac{D}{D'} = 1.5 \Rightarrow 3.5 \text{ dB} \\ |G_{d0}| &= \frac{|V|}{DD'} = 187.5 \text{ V} \Rightarrow 45.5 \text{ dBV} \\ f_0 &= \frac{\omega_0}{2\pi} = \frac{D'}{2\pi\sqrt{LC}} = 400 \text{ Hz} \\ Q &= D'R\sqrt{\frac{C}{L}} = 4 \Rightarrow 12 \text{ dB} \\ f_z &= \frac{\omega_z}{2\pi} = \frac{D'^2R}{2\pi DL} = 2.65 \text{ kHz} \end{aligned} \quad (8.131)$$

The Bode plot of the magnitude and phase of G_{vd} is constructed in Fig. 8.33. The transfer function contains a dc gain of 45.5 dBV, resonant poles at 400 Hz having a Q of 4 \Rightarrow 12 dB, and a right half-plane zero at 2.65 kHz. The resonant poles contribute -180° to the high-frequency phase asymptote, while the right half-plane zero contributes -90° . In addition, the inverting characteristic of the buck-boost converter leads to a 180° phase reversal, not included in Fig. 8.33.

The Bode plot of the magnitude and phase of the line-to-output transfer function G_{vg} is constructed in Fig. 8.34. This transfer function contains the same resonant poles at 400 Hz, but is missing the right half-plane zero. The dc gain G_{g0} is equal to the conversion ratio $M(D)$ of the converter. Again, the 180° phase reversal, caused by the inverting characteristic of the buck-boost converter, is not included in Fig. 8.34.

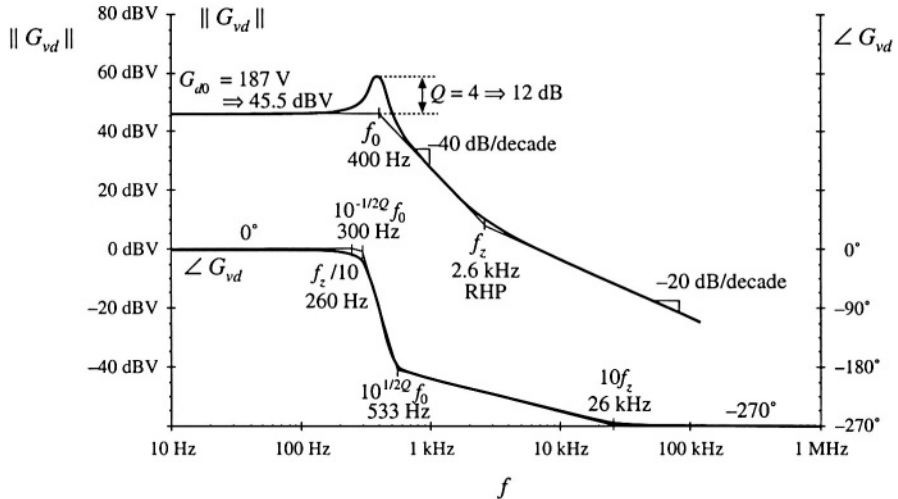


Fig. 8.33 Bode plot of the control-to-output transfer function G_{vd} , buck-boost converter example. Phase reversal owing to output voltage inversion is not included.

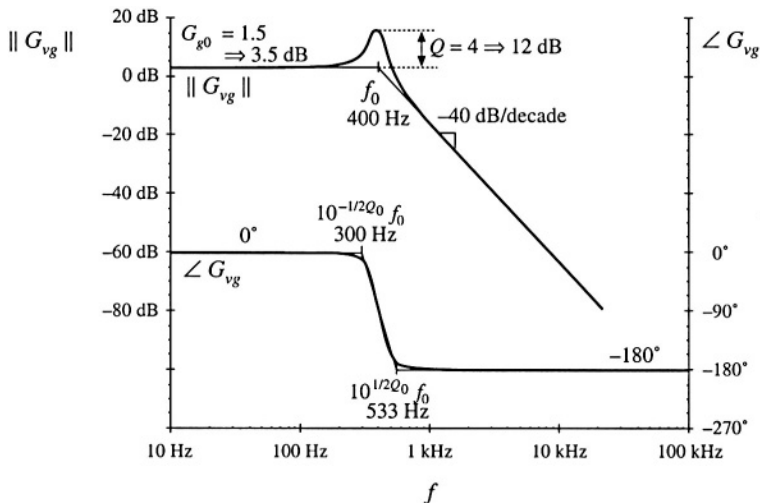


Fig. 8.34 Bode plot of the line-to-output transfer function G_{vg} , buck-boost converter example. Phase reversal owing to output voltage reversal is not included.

Table 8.2 Salient features of the small-signal CCM transfer functions of some basic dc–dc converters

Converter	G_{g0}	G_{d0}	ω_0	Q	ω_z
Buck	D	$\frac{V}{D}$	$\frac{1}{\sqrt{LC}}$	$R \sqrt{\frac{C}{L}}$	∞
Boost	$\frac{1}{D'}$	$\frac{V}{D'}$	$\frac{D'}{\sqrt{LC}}$	$D'R \sqrt{\frac{C}{L}}$	$\frac{D'^2 R}{L}$
Buck-boost	$-\frac{D}{D'}$	$\frac{V}{DD'}$	$\frac{D'}{\sqrt{LC}}$	$D'R \sqrt{\frac{C}{L}}$	$\frac{D'^2 R}{DL}$

8.2.2 Transfer Functions of Some Basic CCM Converters

The salient features of the line-to-output and control-to-output transfer functions of the basic buck, boost, and buck-boost converters are summarized in Table 8.2. In each case, the control-to-output transfer function is of the form

$$G_{vd}(s) = G_{d0} \frac{\left(1 - \frac{s}{\bar{\omega}_z}\right)}{\left(1 + \frac{s}{Q\omega_0} + \left(\frac{s}{\bar{\omega}_0}\right)^2\right)} \quad (8.132)$$

and the line-to-output transfer function is of the form

$$G_{vg}(s) = G_{g0} \frac{1}{1 + \frac{s}{Q\omega_0} + \left(\frac{s}{\bar{\omega}_0}\right)^2} \quad (8.133)$$

The boost and buck-boost converters exhibit control-to-output transfer functions containing two poles and a right half-plane zero. The buck converter $G_{vg}(s)$ exhibits two poles but no zero. The line-to-output transfer functions of all three ideal converters contain two poles and no zeroes.

These results can be easily adapted to transformer-isolated versions of the buck, boost, and buck-boost converters. The transformer has negligible effect on the transfer functions $G_{vg}(s)$ and $G_{vd}(s)$, other than introduction of a turns ratio. For example, when the transformer of the bridge topology is driven symmetrically, its magnetizing inductance does not contribute dynamics to the converter small-signal transfer functions. Likewise, when the transformer magnetizing inductance of the forward converter is reset by the input voltage v_g , as in Fig. 6.23 or 6.28, then it also contributes negligible dynamics. In all transformer-isolated converters based on the buck, boost, and buck-boost converters, the line-to-output transfer function $G_{vg}(s)$ should be multiplied by the transformer turns ratio; the transfer functions (8.132) and (8.133) and the parameters listed in Table 8.2 can otherwise be directly applied.

8.2.3 Physical Origins of the Right Half-Plane Zero in Converters

Figure 8.35 contains a block diagram that illustrates the behavior of the right half-plane zero. At low frequencies, the gain (s/ω_z) has negligible magnitude, and hence $u_{out} \approx u_{in}$. At high frequencies, where the

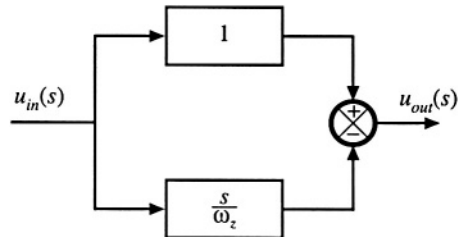


Fig. 8.35 Block diagram having a right half-plane zero transfer function, as in Eq. (8.32), with $\omega_0 = \omega_z$.

magnitude of the gain (s/ω_z) is much greater than 1, $u_{out} \approx -(s/\omega_z)u_{in}$. The negative sign causes a phase reversal at high frequency. The implication for the transient response is that the output initially tends in the opposite direction of the final value.

We have seen that the control-to-output transfer functions of the boost and buck-boost converters, Fig. 8.36, exhibit RHP zeroes. Typical transient response waveforms for a step change in duty cycle are illustrated in Fig. 8.37. For this example, the converter initially operates in equilibrium, at $d = 0.4$ and $d' = 0.6$. Equilibrium inductor current $i_L(t)$, diode current $i_D(t)$, and output voltage $v(t)$ waveforms are illustrated. The average diode current is

$$\langle i_D \rangle_{T_s} = d' \langle i_L \rangle_{T_s} \quad (8.134)$$

By capacitor charge balance, this average diode current is equal to the dc load current when the converter operates in equilibrium. At time $t = t_1$, the duty cycle is increased to 0.6. In consequence, d' decreases to 0.4. The average diode current, given by Eq. (8.134), therefore decreases, and the output capacitor begins to discharge. The output voltage magnitude initially decreases as illustrated.

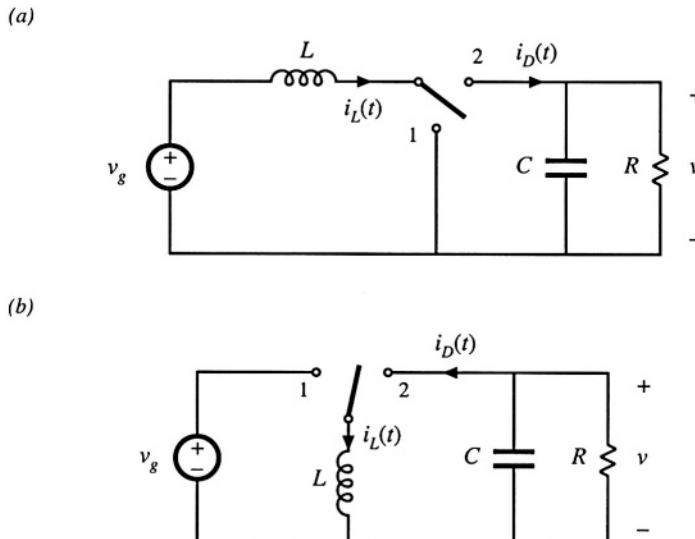


Fig. 8.36 Two basic converters whose CCM control-to-output transfer functions exhibit RHP zeroes: (a) boost, (b) buck-boost.

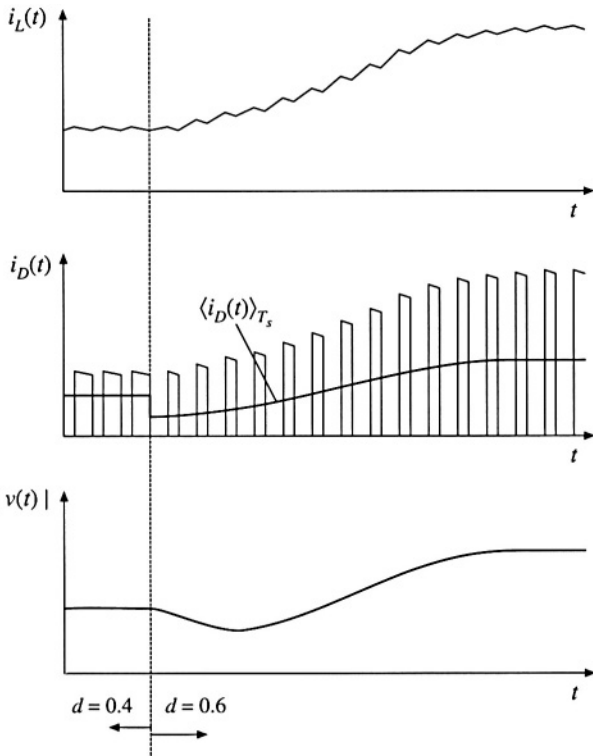


Fig. 8.37 Waveforms of the converters of Fig. 8.36, for a step response in duty cycle. The average diode current and output voltage initially decrease, as predicted by the RHP zero. Eventually, the inductor current increases, causing the average diode current and the output voltage to increase.

The increased duty cycle causes the inductor current to slowly increase, and hence the average diode current eventually exceeds its original $d = 0.4$ equilibrium value. The output voltage eventually increases in magnitude, to the new equilibrium value corresponding to $d = 0.6$.

The presence of a right half-plane zero tends to destabilize wide-bandwidth feedback loops, because during a transient the output initially changes in the wrong direction. The phase margin test for feedback loop stability is discussed in the next chapter; when a RHP zero is present, it is difficult to obtain an adequate phase margin in conventional single-loop feedback systems having wide bandwidth. Prediction of the right half-plane zero, and the consequent explanation of why the feedback loops controlling CCM boost and buck-boost converters tend to oscillate, was one of the early successes of averaged converter modeling.

8.3 GRAPHICAL CONSTRUCTION OF IMPEDANCES AND TRANSFER FUNCTIONS

Often, we can draw approximate Bode diagrams by inspection, without large amounts of messy algebra and the inevitable associated algebra mistakes. A great deal of insight can be gained into the operation of the circuit using this method. It becomes clear which components dominate the circuit response at various frequencies, and so suitable approximations become obvious. Analytical expressions for the approximate corner frequencies and asymptotes can be obtained directly. Impedances and transfer functions of quite complicated networks can be constructed. Thus insight can be gained, so that the design engineer

can modify the circuit to obtain a desired frequency response.

The graphical construction method, also known as “doing algebra on the graph,” involves use of a few simple rules for combining the magnitude Bode plots of impedances and transfer functions.

8.3.1 Series Impedances: Addition of Asymptotes

A series connection represents the addition of impedances. If the Bode diagrams of the individual impedance magnitudes are known, then the asymptotes of the series combination are found by simply taking the largest of the individual impedance asymptotes. In many cases, the result is exact. In other cases, such as when the individual asymptotes have the same slope, then the result is an approximation; nonetheless, the accuracy of the approximation can be quite good.

Consider the series-connected $R-C$ network of Fig. 8.38. It is desired to construct the magnitude asymptotes of the total series impedance $Z(s)$, where

$$Z(s) = R + \frac{1}{sC} \quad (8.135)$$

Let us first sketch the magnitudes of the individual impedances. The $10\ \Omega$ resistor has an impedance magnitude of $10\ \Omega \Rightarrow 20\ \text{dB}\Omega$. This value is independent of frequency, and is given in Fig. 8.39. The capacitor has an impedance magnitude of $1/\omega C$. This quantity varies inversely with ω , and hence its magnitude Bode plot is a line with slope $-20\ \text{dB}/\text{decade}$. The line passes through $1\ \Omega \Rightarrow 0\ \text{dB}\Omega$ at the angular frequency ω where

$$\frac{1}{\omega C} = 1\ \Omega \quad (8.136)$$

that is, at

$$\omega = \frac{1}{(1\ \Omega)C} = \frac{1}{(1\ \Omega)(10^{-6}\ \text{F})} = 10^6\ \text{rad/sec} \quad (8.137)$$

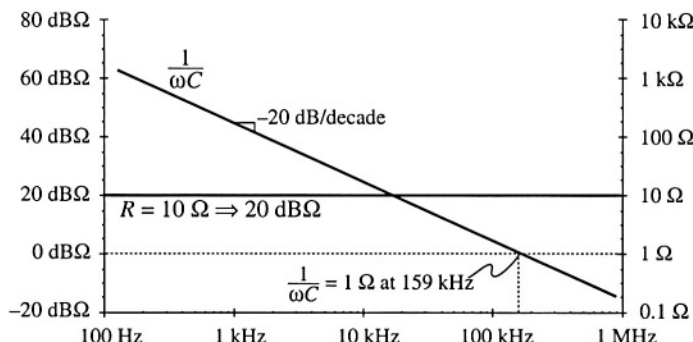


Fig. 8.38 Series $R-C$ network example.

Fig. 8.39 Impedance magnitudes of the individual elements in the network of Fig. 8.38.

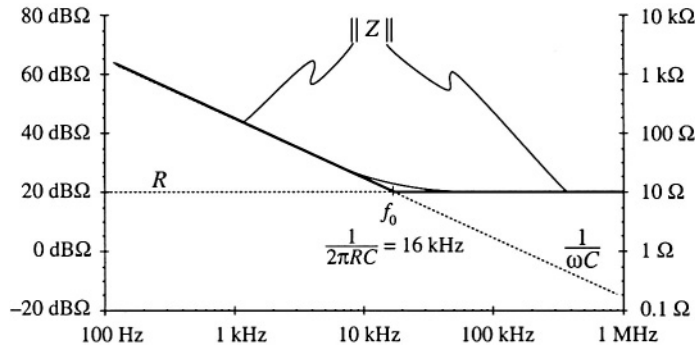


Fig. 8.40 Construction of the composite asymptotes of $\| Z \|$. The asymptotes of the series combination can be approximated by simply selecting the larger of the individual resistor and capacitor asymptotes.

In terms of frequency f , this occurs at

$$f = \frac{\omega}{2\pi} = \frac{10^6}{2\pi} = 159 \text{ kHz} \quad (8.138)$$

So the capacitor impedance magnitude is a line with slope -20 dB/dec , and which passes through 0 dBΩ at 159 kHz , as shown in Fig. 8.39. It should be noted that, for simplicity, the asymptotes in Fig. 8.39 have been labeled R and $1/\omega C$. But to draw the Bode plot, we must actually plot dBΩ ; for example, $20 \log_{10}(R/1 \Omega)$ and $20 \log_{10}((1/\omega C)/1 \Omega)$.

Let us now construct the magnitude of $Z(s)$, given by Eq. (8.135). The magnitude of Z can be approximated as follows:

$$\| Z(j\omega) \| = \left| R + \frac{1}{j\omega C} \right| \approx \begin{cases} R & \text{for } R \gg 1/\omega C \\ \frac{1}{\omega C} & \text{for } R \ll 1/\omega C \end{cases} \quad (8.139)$$

The asymptotes of the series combination are simply the larger of the individual resistor and capacitor asymptotes, as illustrated by the heavy lines in Fig. 8.40. For this example, these are in fact the exact asymptotes of $\| Z \|$. In the limiting case of zero frequency (dc), then the capacitor tends to an open circuit. The series combination is then dominated by the capacitor, and the exact function tends asymptotically to the capacitor impedance magnitude. In the limiting case of infinite frequency, then the capacitor tends to a short circuit, and the total impedance becomes simply R . So the R and $1/\omega C$ lines are the exact asymptotes for this example.

The corner frequency f_0 , where the asymptotes intersect, can now be easily deduced. At angular frequency $\omega_0 = 2\pi f_0$, the two asymptotes are equal in value:

$$\frac{1}{\omega_0 C} = R \quad (8.140)$$

Solution for ω_0 and f_0 leads to:

$$\begin{aligned}\omega_0 &= \frac{1}{RC} = \frac{1}{(10\Omega)(10^{-6}F)} = 10^5 \text{ rad/sec} \\ f_0 &= \frac{\omega_0}{2\pi} = \frac{1}{2\pi RC} = 16 \text{ kHz}\end{aligned}\quad (8.141)$$

So if we can write analytical expressions for the asymptotes, then we can equate the expressions to find analytical expressions for the corner frequencies where the asymptotes intersect.

The deviation of the exact curve from the asymptotes follows all of the usual rules. The slope of the asymptotes changes by +20 dB/decade at the corner frequency f_0 (i.e., from $-20 \text{ dB}\Omega/\text{decade}$ to $0 \text{ dB}\Omega/\text{decade}$), and hence there is a zero at $f = f_0$. So the exact curve deviates from the asymptotes by +3 dBΩ at $f = f_0$, and by +1 dBΩ at $f = 2f_0$ and at $f = f_0/2$.

8.3.2 Series Resonant Circuit Example

As a second example, let us construct the magnitude asymptotes for the series $R-L-C$ circuit of Fig. 8.41. The series impedance $Z(s)$ is

$$Z(s) = R + sL + \frac{1}{sC} \quad (8.142)$$

The magnitudes of the individual resistor, inductor, and capacitor asymptotes are plotted in Fig. 8.42, for the values

$$\begin{aligned}R &= 1 \text{ k}\Omega \\ L &= 1 \text{ mH} \\ C &= 0.1 \mu\text{F}\end{aligned}\quad (8.143)$$

The series impedance $Z(s)$ is dominated by the capacitor at low frequency, by the resistor at mid frequencies, and by the inductor at high frequencies, as illustrated by the bold line in Fig. 8.42. The impedance $Z(s)$ contains a zero at angular frequency ω_1 , where the capacitor and resistor asymptotes intersect. By equating the expressions for the resistor and capacitor asymptotes, we can find ω_1 :

$$R = \frac{1}{\omega_1 C} \Rightarrow \omega_1 = \frac{1}{RC} \quad (8.144)$$

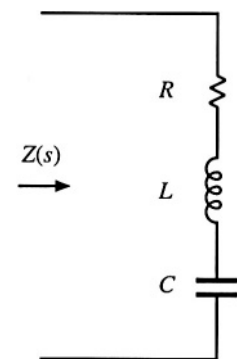
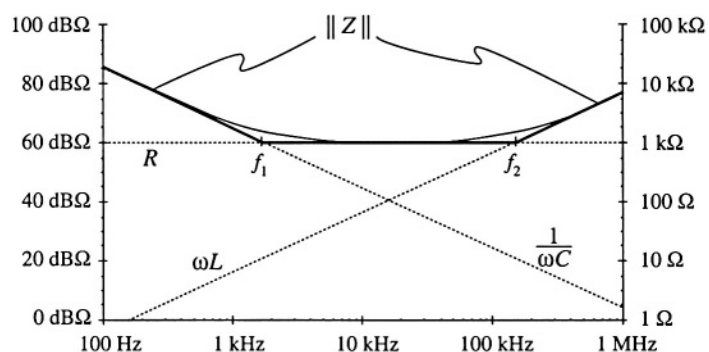


Fig. 8.41 Series $R-L-C$ network example.

Fig. 8.42 Graphical construction of $\|Z\|$ of the series $R-L-C$ network of Fig. 8.41, for the element values specified by Eq. (8.143).



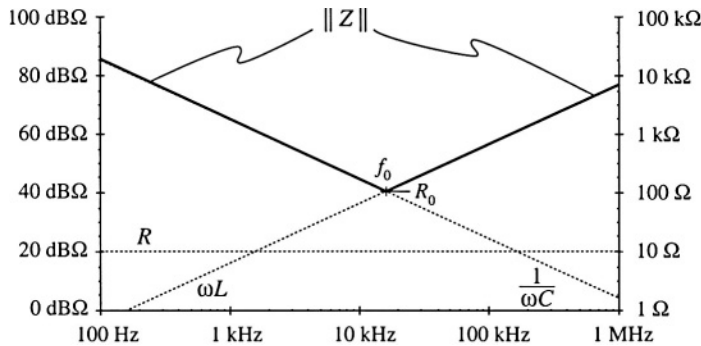


Fig. 8.43 Graphical construction of impedance asymptotes for the series R-L-C network example, with R decreased to 10Ω .

A second zero occurs at angular frequency ω_2 , where the inductor and resistor asymptotes intersect. Upon equating the expressions for the resistor and inductor asymptotes at ω_2 , we obtain the following:

$$R = \omega_2 L \Rightarrow \omega_2 = \frac{R}{L} \quad (8.145)$$

So simple expressions for all important features of the magnitude Bode plot of $Z(s)$ can be obtained directly. It should be noted that Eqs. (8.144) and (8.145) are approximate, rather than exact, expressions for the corner frequencies ω_1 and ω_2 . Equations (8.144) and (8.145) coincide with the results obtained via the low- Q approximation of Section 8.1.7.

Next, suppose that the value of R is decreased to 10Ω . As R is reduced in value, the approximate corner frequencies ω_1 and ω_2 move closer together until, at $R = 100 \Omega$, they are both 100 krad/sec . Reducing R further in value causes the asymptotes to become independent of the value of R , as illustrated in Fig. 8.43 for $R = 10 \Omega$. The $\|Z\|$ asymptotes now switch directly from ωL to $1/\omega C$.

So now there are two zeroes at $\omega = \omega_0$. At corner frequency ω_0 , the inductor and capacitor asymptotes are equal in value. Hence,

$$\omega_0 L = \frac{1}{\omega_0 C} = R_0 \quad (8.146)$$

Solution for the angular corner frequency ω_0 leads to

$$\omega_0 = \frac{1}{\sqrt{LC}} \quad (8.147)$$

At $\omega = \omega_0$, the inductor and capacitor impedances both have magnitude R_0 , called the characteristic impedance.

Since there are two zeroes at $\omega = \omega_0$, there is a possibility that the two poles could be complex conjugates, and that peaking could occur in the vicinity of $\omega = \omega_0$. So let us investigate what the actual curve does at $\omega = \omega_0$. The actual value of the series impedance $Z(j\omega_0)$ is

$$Z(j\omega_0) = R + j\omega_0 L + \frac{1}{j\omega_0 C} \quad (8.148)$$

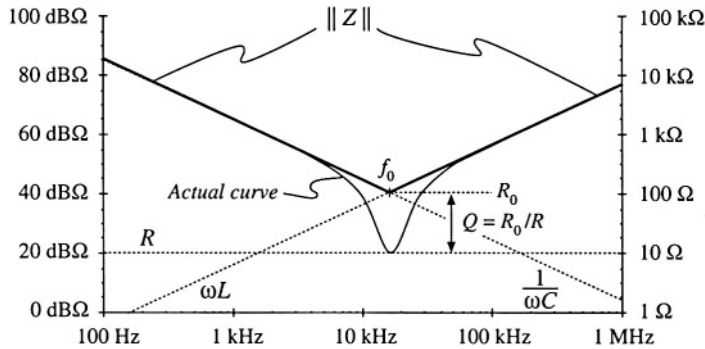


Fig. 8.44 Actual impedance magnitude (solid line) for the series resonant $R-L-C$ example. The inductor and capacitor impedances cancel out at $f=f_0$, and hence $Z(j\omega_0)=R$.

Substitution of Eq. (8.146) into Eq. (8.147) leads to

$$Z(j\omega_0) = R + jR_0 + \frac{R_0}{j} = R + jR_0 - jR_0 = R \quad (8.149)$$

At $\omega = \omega_0$, the inductor and capacitor impedances are equal in magnitude but opposite in phase. Hence, they exactly cancel out in the series impedance, and we are left with $Z(j\omega_0) = R$, as illustrated in Fig. 8.44. The actual curve in the vicinity of the resonance at $\omega = \omega_0$ can deviate significantly from the asymptotes, because its value is determined by R rather than ωL or $1/\omega C$.

We know from Section 8.1.6 that the deviation of the actual curve from the asymptotes at $\omega = \omega_0$ is equal to Q . From Fig. 8.44, one can see that

$$|Q|_{dB} = |R_0|_{dB\Omega} - |R|_{dB\Omega} \quad (8.150)$$

or,

$$Q = \frac{R_0}{R} \quad (8.151)$$

Equations (8.146) to (8.151) are exact results for the series resonant circuit.

The practice of adding asymptotes by simply selecting the larger asymptote can be applied to transfer functions as well as impedances. For example, suppose that we have already constructed the magnitude asymptotes of two transfer functions, G_1 and G_2 , and we wish to find the asymptotes of $G = G_1 + G_2$. At each frequency, the asymptote for G can be approximated by simply selecting the larger of the asymptotes for G_1 and G_2 :

$$G = G_1 + G_2 \approx \begin{cases} G_1, & |G_1| \gg |G_2| \\ G_2, & |G_2| \gg |G_1| \end{cases} \quad (8.152)$$

Corner frequencies can be found by equating expressions for asymptotes as illustrated in the preceding examples. In the next chapter, we will see that this approach yields a simple and powerful method for determining the closed-loop transfer functions of feedback systems.

8.3.3 Parallel Impedances: Inverse Addition of Asymptotes

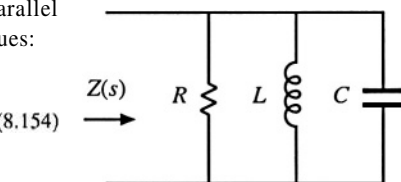
A parallel combination represents inverse addition of impedances:

$$Z_{par} = \frac{1}{\frac{1}{Z_1} + \frac{1}{Z_2} + \dots} \quad (8.153)$$

If the asymptotes of the individual impedances Z_1, Z_2, \dots , are known, then the asymptotes of the parallel combination Z_{par} can be found by simply selecting the smallest individual impedance asymptote. This is true because the smallest impedance will have the largest inverse, and will dominate the inverse sum. As in the case of the series impedances, this procedure will often yield the exact asymptotes of Z_{par} .

Let us construct the magnitude asymptotes for the parallel $R-L-C$ network of Fig. 8.45, using the following element values:

$$\begin{aligned} R &= 10 \Omega \\ L &= 1 \text{ mH} \\ C &= 0.1 \mu\text{F} \end{aligned} \quad (8.154)$$



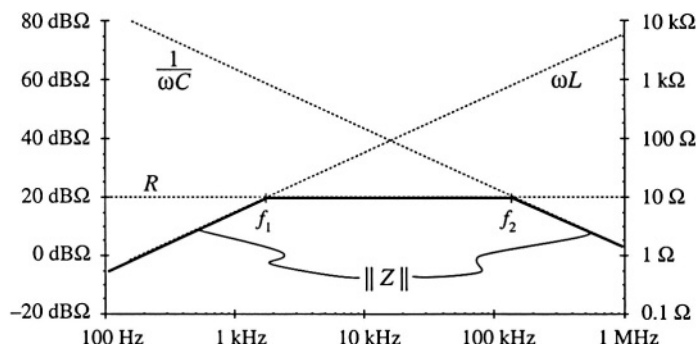
Impedance magnitudes of the individual elements are illustrated in Fig. 8.45 Parallel $R-L-C$ network Fig. 8.46. The asymptotes for the total parallel impedance Z are example.

approximated by simply selecting the smallest individual element impedance, as shown by the heavy line in Fig. 8.46. So the parallel impedance is dominated by the inductor at low frequency, by the resistor at mid frequencies, and by the capacitor at high frequency. Approximate expressions for the angular corner frequencies are again found by equating asymptotes:

$$\begin{aligned} \text{at } \omega = \omega_1, \quad R = \omega_1 L \Rightarrow \omega_1 = \frac{R}{L} \\ \text{at } \omega = \omega_2, \quad R = \frac{1}{\omega_2 C} \Rightarrow \omega_2 = \frac{1}{RC} \end{aligned} \quad (8.155)$$

These expressions could have been obtained by conventional analysis, combined with the low- Q approximation of Section 8.1.7.

Fig. 8.46 Construction of the composite asymptotes of $\| Z \|$, for the parallel $R-L-C$ example. The asymptotes of the parallel combination can be approximated by simply selecting the smallest of the individual resistor, inductor, and capacitor asymptotes.



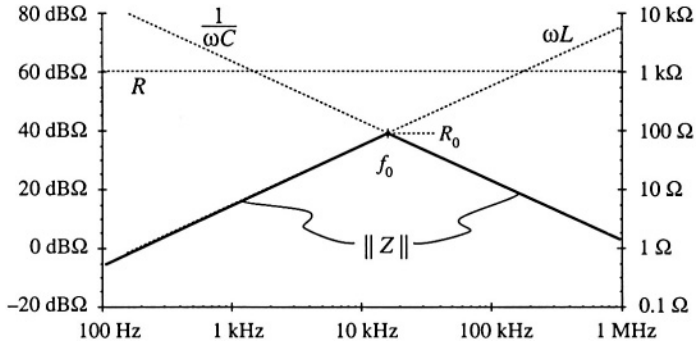


Fig. 8.47 Graphical construction of impedance asymptotes for the parallel R - L - C example, with R increased to $1\text{ k}\Omega$.

8.3.4 Parallel Resonant Circuit Example

Figure 8.47 illustrates what happens when the value of R in the parallel R - L - C network is increased to $1\text{ k}\Omega$. The asymptotes for $\|Z\|$ then become independent of R , and change directly from ωL to $1/\omega C$ at angular frequency ω_0 . The corner frequency ω_0 is now the frequency where the inductor and capacitor asymptotes have equal value:

$$\omega_0 L = \frac{1}{\omega_0 C} = R_0 \quad (8.156)$$

which implies that

$$\omega_0 = \frac{1}{\sqrt{LC}} \quad (8.157)$$

At $\omega = \omega_0$, the slope of the asymptotes of $\|Z\|$ changes from $+20\text{ dB/decade}$ to -20 dB/decade , and hence there are two poles. We should investigate whether peaking occurs, by determining the exact value of $\|Z\|$ at $\omega = \omega_0$, as follows:

$$Z(j\omega_0) = R \| j\omega_0 L \| \frac{1}{j\omega_0 C} = \frac{1}{\frac{1}{R} + \frac{1}{j\omega_0 L} + j\omega_0 C} \quad (8.158)$$

Substitution of Eq. (8.156) into (8.158) yields

$$Z(j\omega_0) = \frac{1}{\frac{1}{R} + \frac{1}{jR_0} + \frac{j}{R_0}} = \frac{1}{\frac{1}{R} - \frac{j}{R_0} + \frac{j}{R_0}} = R \quad (8.159)$$

So at $\omega = \omega_0$, the impedances of the inductor and capacitor again cancel out, and we are left with $Z(j\omega_0) = R$. The values of L and C determine the values of the asymptotes, but R determines the value of the actual curve at $\omega = \omega_0$.

The actual curve is illustrated in 8.48. The deviation of the actual curve from the asymptotes at $\omega = \omega_0$ is

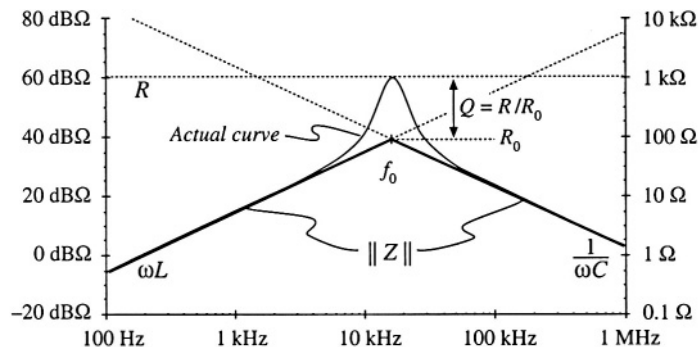


Fig. 8.48 Actual impedance magnitude (solid line) for the parallel $R-L-C$ example. The inductor and capacitor impedances cancel out at $f = f_0$, and hence $Z(j\omega_0) = R$.

$$|Q|_{dB} = |R|_{dB\Omega} - |R_0|_{dB\Omega} \quad (8.160)$$

or,

$$Q = \frac{R}{R_0} \quad (8.161)$$

Equations (8.156) to (8.161) are exact results for the parallel resonant circuit.

The graphical construction method for impedance magnitudes is well known, and *reactance paper* can be purchased commercially. As illustrated in Fig. 8.49, the magnitudes of the impedances of various inductances, capacitances, and resistances are plotted on semilogarithmic axes. Asymptotes for the impedances of $R-L-C$ networks can be sketched directly on these axes, and numerical values of corner frequencies can then be graphically determined.

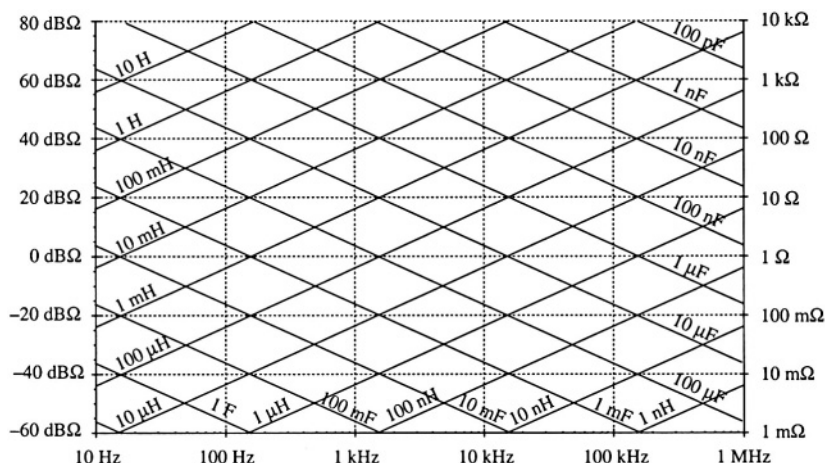


Fig. 8.49 “Reactance paper”: an aid for graphical construction of impedances, with the magnitudes of various inductive, capacitive, and resistive impedances preplotted.

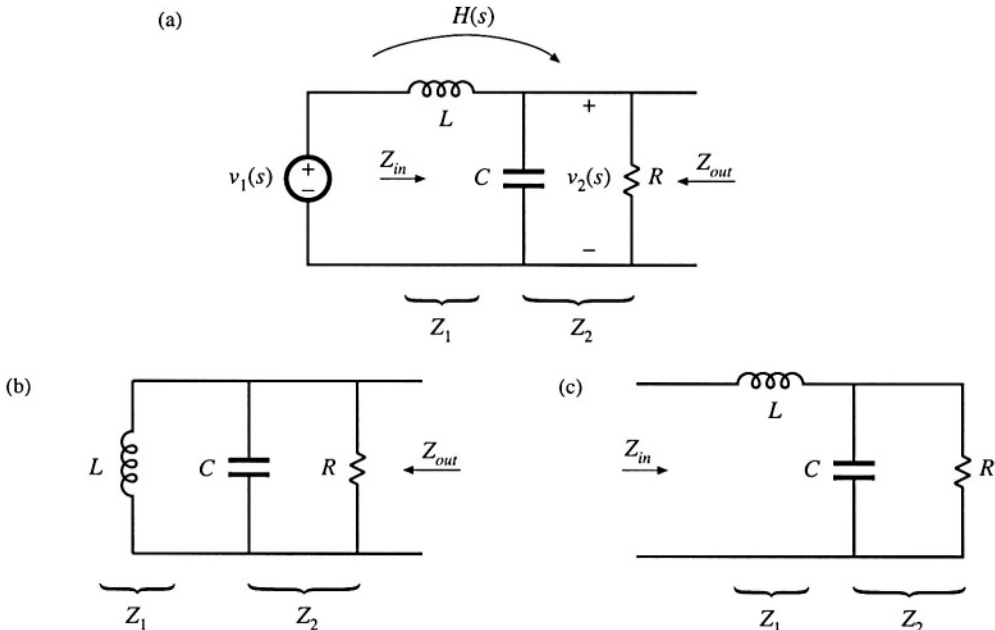


Fig. 8.50 Two-pole low-pass filter based on voltage divider circuit: (a) transfer function $H(s)$, (b) determination of Z_{out} by setting independent sources to zero, (c) determination of $Z_{in}(s)$.

8.3.5 Voltage Divider Transfer Functions: Division of Asymptotes

Usually, we can express transfer functions in terms of impedances—for example, as the ratio of two impedances. If we can construct these impedances as described in the previous sections, then we can divide to construct the transfer function. In this section, construction of the transfer function $H(s)$ of the two-pole $R-L-C$ low-pass filter (Fig. 8.50) is discussed in detail. A filter of this form appears in the canonical model for two-pole converters, and the results of this section are applied in the converter examples of the next section.

The familiar voltage divider formula shows that the transfer function of this circuit can be expressed as the ratio of impedances Z_2/Z_{in} , where $Z_{in} = Z_1 + Z_2$ is the network input impedance:

$$\frac{\hat{v}_2(s)}{\hat{v}_1(s)} = \frac{Z_2}{Z_1 + Z_2} = \frac{Z_2}{Z_{in}} \quad (8.162)$$

For this example, $Z_1(s) = sL$, and $Z_2(s)$ is the parallel combination of R and $1/sC$. Hence, we can find the transfer function asymptotes by constructing the asymptotes of Z_2 and of the series combination represented by Z_{in} , and then dividing. Another approach, which is easier to apply in this example, is to multiply the numerator and denominator of Eq. (8.162) by Z_1 :

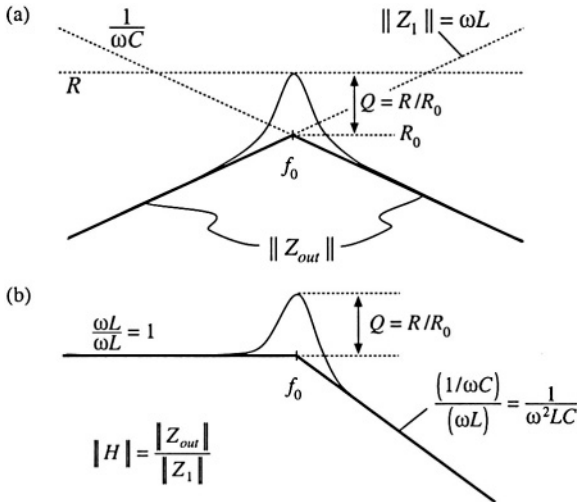


Fig. 8.51 Graphical construction of H and Z_{out} of the voltage divider circuit: (a) output impedance Z_{out} ; (b) transfer function H .

$$\frac{\hat{v}_2(s)}{\hat{v}_1(s)} = \frac{Z_2 Z_1}{Z_1 + Z_2} \frac{1}{Z_1} = \frac{Z_{out}}{Z_1} \quad (8.163)$$

where $Z_{out} = Z_1 \parallel Z_2$ is the output impedance of the voltage divider. So another way to construct the voltage divider transfer function is to first construct the asymptotes for Z_1 and for the parallel combination represented by Z_{out} , and then divide. This method is useful when the parallel combination $Z_1 \parallel Z_2$ is easier to construct than the series combination $Z_1 + Z_2$. It often gives a different approximate result, which may be more (or sometimes less) accurate than the result obtained using Z_{in} .

The output impedance Z_{out} in Fig. 8.50(b) is

$$Z_{out}(s) = R \parallel \frac{1}{sC} \parallel sL \quad (8.164)$$

The impedance of the parallel $R-L-C$ network is constructed in Section 8.3.3, and is illustrated in Fig. 8.51(a) for the high- Q case.

According to Eq. (8.163), the voltage divider transfer function magnitude is $\|H\| = \|Z_{out}\| / \|Z_1\|$. This quantity is constructed in Fig. 8.51(b). For $\omega < \omega_0$, the asymptote of $\|Z_{out}\|$ coincides with $\|Z_1\|$: both are equal to ωL . Hence, the ratio is $\|Z_{out}\| / \|Z_1\| = 1$. For $\omega > \omega_0$, the asymptote of $\|Z_{out}\|$ is $1/\omega C$, while $\|Z_1\|$ is equal to ωL . The ratio then becomes $\|Z_{out}\| / \|Z_1\| = 1/\omega^2 LC$, and hence the high-

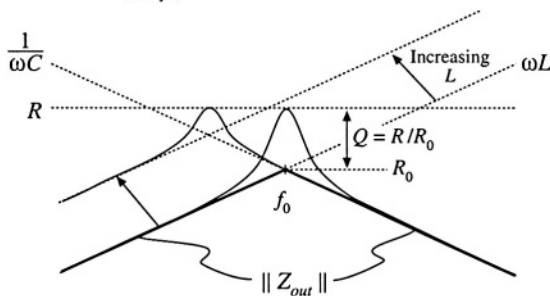


Fig. 8.52 Effect of increasing L on the output impedance asymptotes, corner frequency, and Q -factor.

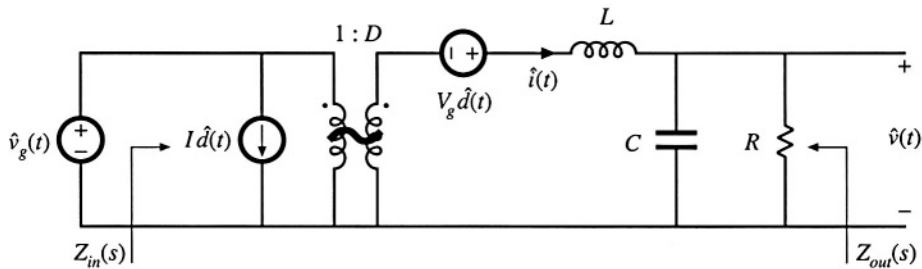


Fig. 8.53 Small-signal model of the buck converter, with input impedance $Z_{in}(s)$ and output impedance $Z_{out}(s)$ explicitly defined.

frequency asymptote has a -40 dB/decade slope. At $\omega = \omega_0$, $\|Z_{out}\|$ has exact value R , while $\|Z_1\|$ has exact value R_0 . The ratio is then $\|H(j\omega_0)\| = \|Z_{out}(j\omega_0)\|/\|Z_1(j\omega_0)\| = R/R_0 = Q$. So the filter transfer function H has the same ω_0 and Q as the impedance Z_{out} .

It now becomes obvious how variations in element values affect the salient features of the transfer function and output impedance. For example, the effect of increasing L is illustrated in Fig. 8.52. This causes the angular resonant frequency ω_0 to be reduced, and also reduces the Q -factor.

8.4 GRAPHICAL CONSTRUCTION OF CONVERTER TRANSFER FUNCTIONS

The small-signal equivalent circuit model of the buck converter, derived in Chapter 7, is reproduced in Fig. 8.53. Let us construct the transfer functions and terminal impedances of this converter, using the graphical approach of the previous section.

The output impedance $Z_{out}(s)$ is found with the $\hat{d}(s)$ and $\hat{v}_g(s)$ sources set to zero; the circuit of Fig. 8.54(a) is then obtained. This model coincides with the parallel $R-L-C$ circuit analyzed in Sections 8.3.3 and 8.3.4. As illustrated in Fig. 8.54(b), the output impedance is dominated by the inductor at low frequency, and by the capacitor at high frequency. At the resonant frequency f_0 , given by

$$f_0 = \frac{1}{2\pi\sqrt{LC}} \quad (8.165)$$

the output impedance is equal to the load resistance R . The Q -factor of the circuit is equal to

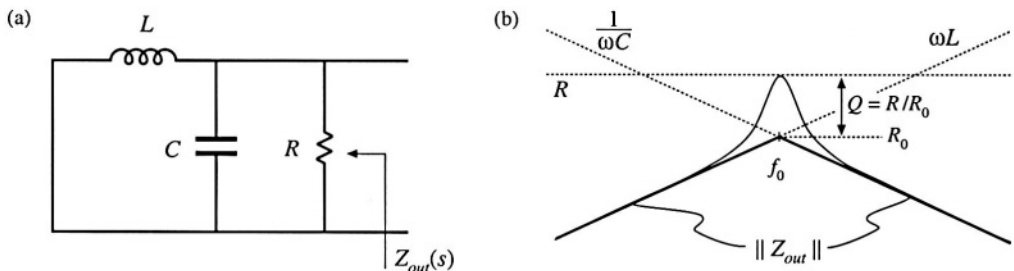


Fig. 8.54 Construction of buck converter output impedance $Z_{out}(s)$: (a) circuit model; (b) impedance asymptotes.

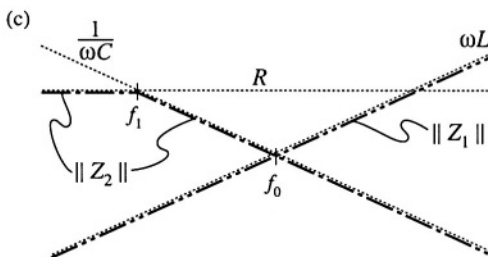
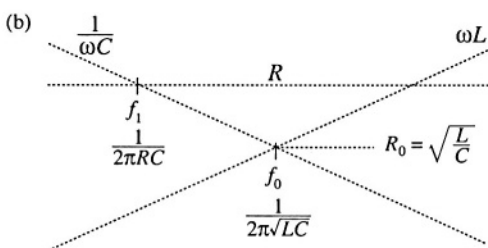
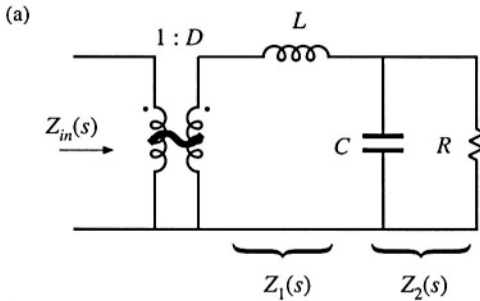
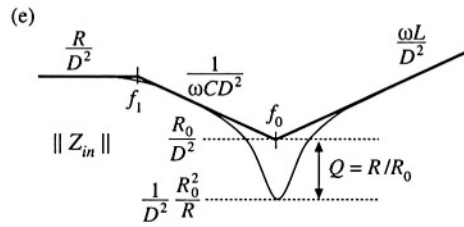
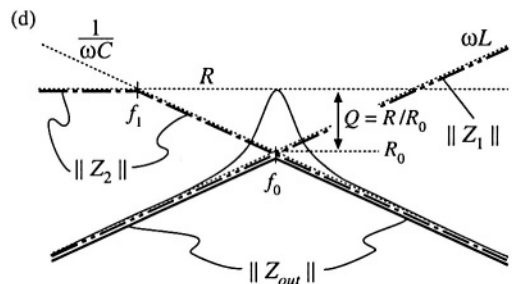


Fig. 8.55 Construction of the input impedance $Z_{in}(s)$ for the buck converter: (a) circuit model; (b) the individual resistor, inductor, and capacitor impedance magnitudes; (c) construction of the impedance magnitudes $\|Z_1\|$ and $\|Z_2\|$; (d) construction of $\|Z_{out}\|$; (e) final result $\|Z_{in}\|$.



$$Q = \frac{R}{R_0} \quad (8.166)$$

where

$$R_0 = \omega_0 L = \frac{1}{\omega_0 C} = \sqrt{\frac{L}{C}} \quad (8.167)$$

Thus, the circuit is lightly damped (high Q) at light load, where the value of R is large.

The converter input impedance $Z_{in}(s)$ is also found with the $\hat{d}(s)$ and $\hat{v}_g(s)$ sources set to zero, as illustrated in Fig. 8.55(a). The input impedance is referred to the primary side of the 1:D transformer, and is equal to

$$Z_{in}(s) = \frac{1}{D^2} [Z_1(s) + Z_2(s)] \quad (8.168)$$

where

$$Z_1(s) = sL \quad (8.169)$$

and

$$Z_2(s) = R \parallel \frac{1}{sC} \quad (8.170)$$

We begin construction of the impedance asymptotes corresponding to Eqs. (8.168) to (8.170) by constructing the individual resistor, capacitor, and inductor impedances as in Fig. 8.55(b). The impedances in Fig. 8.55 are constructed for the case $R > R_0$. As illustrated in Fig. 8.55(c), $\| Z_1 \|$ coincides with the inductor reactance ωL . The impedance $\| Z_2 \|$ is asymptotic to resistance R at low frequencies, and to the capacitor reactance $1/\omega C$ at high frequency. The resistor and capacitor asymptotes intersect at corner frequency f_1 , given by

$$f_1 = \frac{1}{2\pi RC} \quad (8.171)$$

According to Eq. (8.168), the input impedance $Z_{in}(s)$ is equal to the series combination of $Z_1(s)$ and $Z_2(s)$, divided by the square of the turns ratio D . The asymptotes for the series combination $[Z_1(s) + Z_2(s)]$ are found by selecting the larger of the $\| Z_1 \|$ and $\| Z_2 \|$ asymptotes. The $\| Z_1 \|$ and $\| Z_2 \|$ asymptotes intersect at frequency f_0 , given by Eq. (8.165). It can be seen from Fig. 8.55(c) that the series combination is dominated by Z_2 for $f < f_0$, and by Z_1 for $f > f_0$. Upon scaling the $[Z_1(s) + Z_2(s)]$ asymptotes by the factor $1/D^2$, the input impedance asymptotes of Fig. 8.55(e) are obtained.

The zeroes of $Z_{in}(s)$, at frequency f_0 , have the same Q -factor as the poles of $Z_{out}(s)$ [Eq. (8.166)]. One way to see that this is true is to note that the output impedance can be expressed as

$$Z_{out}(s) = \frac{Z_1(s)Z_2(s)}{Z_1(s) + Z_2(s)} = \frac{Z_1(s)Z_2(s)}{D^2 Z_{in}(s)} \quad (8.172)$$

Hence, we can relate $Z_{out}(s)$ to $Z_{in}(s)$ as follows:

$$Z_{in}(s) = \frac{1}{D^2} \frac{Z_1(s)Z_2(s)}{Z_{out}(s)} \quad (8.173)$$

The impedances $\| Z_1 \|$, $\| Z_2 \|$, and $\| Z_{out} \|$ are illustrated in Fig. 8.55(d). At the resonant frequency $f = f_0$, impedance Z_1 has magnitude R_0 and impedance Z_2 has magnitude approximately equal to R_0 . The output impedance Z_{out} has magnitude R . Hence, Eq. (8.173) predicts that the input impedance has the magnitude

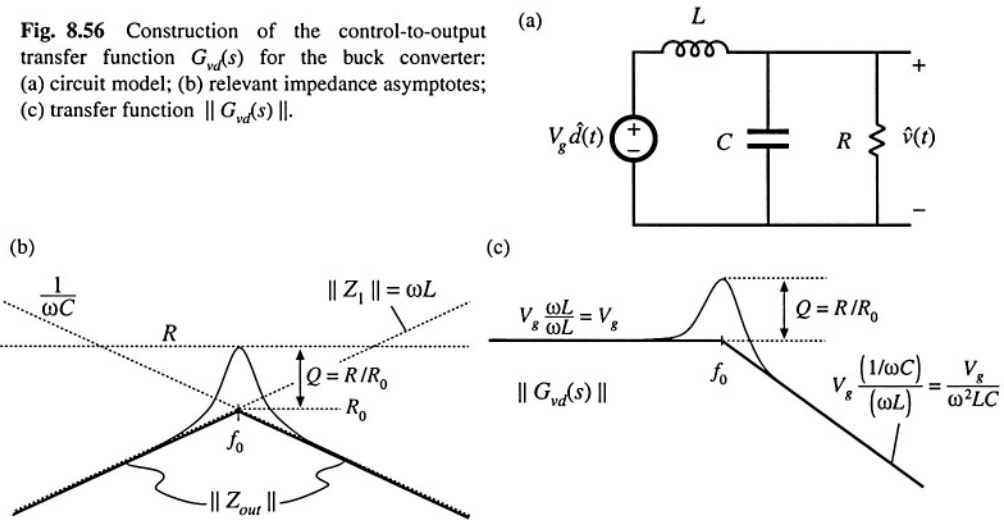
$$\| Z_{in} \| \approx \frac{1}{D^2} \frac{R_0 R_0}{R} \quad \text{at } f = f_0 \quad (8.174)$$

At $f = f_0$, the asymptotes of the input impedance have magnitude R_0/D^2 . The deviation from the asymptotes is therefore equal to $Q = R/R_0$, as illustrated in Fig. 8.55(e).

The control-to-output transfer function $G_{vd}(s)$ is found with the $\hat{v}_g(s)$ source set to zero, as in Fig. 8.56(a). This circuit coincides with the voltage divider analyzed in Section 8.3.5. Hence, $G_{vd}(s)$ can be expressed as

$$G_{vd}(s) = V_g \frac{Z_{out}(s)}{Z_1(s)} \quad (8.175)$$

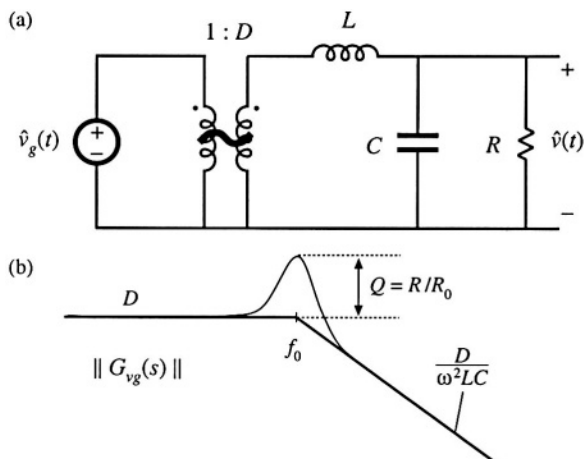
Fig. 8.56 Construction of the control-to-output transfer function $G_{vd}(s)$ for the buck converter:
 (a) circuit model; (b) relevant impedance asymptotes;
 (c) transfer function $\| G_{vd}(s) \|$.



The quantities $\| Z_{out} \|$ and $\| Z_1 \|$ are constructed in Fig. 8.56(b). According to Eq. (8.175), we can construct $\| G_{vd}(s) \|$ by finding the ratio of $\| Z_{out} \|$ and $\| Z_1 \|$, and then scaling the result by V_g . For $f < f_0$, $\| Z_{out} \|$ and $\| Z_1 \|$ are both equal to ωL and hence $\| Z_{out} \| / \| Z_1 \|$ is equal to 1. As illustrated in Fig. 8.56(c), the low-frequency asymptote of $\| G_{vd}(s) \|$ has value V_g . For $f > f_0$, $\| Z_{out} \|$ has asymptote $1/\omega C$, and $\| Z_1 \|$ is equal to ωL . Hence, $\| Z_{out} \| / \| Z_1 \|$ has asymptote $1/\omega^2 LC$, and the high-frequency asymptote of $\| G_{vd}(s) \|$ is equal to $V_g/\omega^2 LC$. The Q -factor of the two poles at $f = f_0$ is again equal to R/R_0 .

The line-to-output transfer function $G_{vg}(s)$ is found with the $\hat{d}(s)$ sources set to zero, as in Fig. 8.57(a). This circuit contains the same voltage divider as in Fig. 8.56, and additionally contains the $1:D$ transformer. The transfer function $G_{vg}(s)$ can be expressed as

Fig. 8.57 The line-to-output transfer function $G_{vg}(s)$ for the buck converter:
 (a) circuit model; (b) magnitude asymptotes.



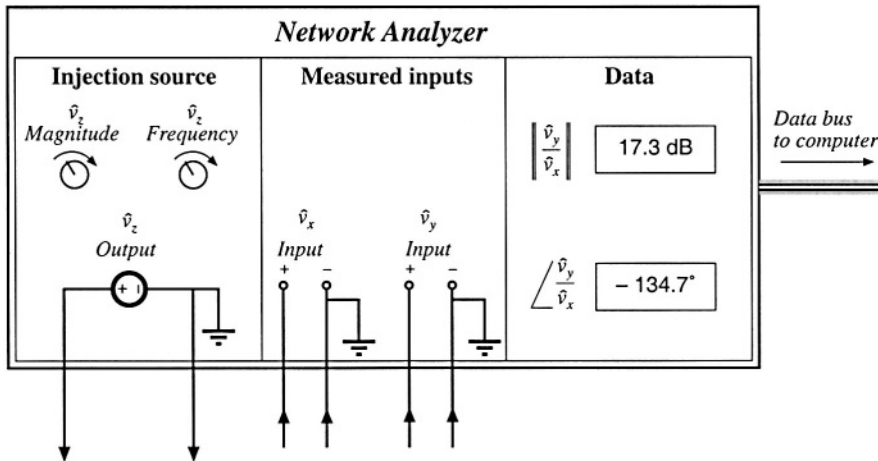


Fig. 8.58 Key features and functions of a network analyzer: sinusoidal source of controllable amplitude and frequency, two inputs, and determination of relative magnitude and phase of the input components at the injection frequency.

$$G_{v_R}(s) = D \frac{Z_{out}(s)}{Z_i(s)} \quad (8.176)$$

This expression is similar to Eq. (8.175), except for the scaling factor of D . Therefore, the line-to-output transfer function of Fig. 8.57(b) has the same shape as the control-to-output transfer function $G_{v_R}(s)$.

8.5 MEASUREMENT OF AC TRANSFER FUNCTIONS AND IMPEDANCES

It is good engineering practice to measure the transfer functions of prototype converters and converter systems. Such an exercise can verify that the system has been correctly modeled and designed. Also, it is often useful to characterize individual circuit elements through measurement of their terminal impedances.

Small-signal ac magnitude and phase measurements can be made using an instrument known as a network analyzer, or frequency response analyzer. The key inputs and outputs of a basic network analyzer are illustrated in Fig. 8.58. The network analyzer provides a sinusoidal output voltage \hat{v}_z of controllable amplitude and frequency. This signal can be injected into the system to be measured, at any desired location. The network analyzer also has two (or more) inputs, \hat{v}_x and \hat{v}_y . The return electrodes of \hat{v}_z , \hat{v}_y , and \hat{v}_x are internally connected to earth ground. The network analyzer performs the function of a narrowband tracking voltmeter: it measures the components of \hat{v}_x and \hat{v}_y at the injection frequency, and displays the magnitude and phase of the quantity \hat{v}_y/\hat{v}_x . The narrowband tracking voltmeter feature is essential for switching converter measurements; otherwise, switching ripple and noise corrupt the desired sinusoidal signals and make accurate measurements impossible [3]. Modern network analyzers can automatically sweep the frequency of the injection source \hat{v}_z to generate magnitude and phase Bode plots of the transfer function \hat{v}_y/\hat{v}_x .

A typical test setup for measuring the transfer function of an amplifier is illustrated in Fig. 8.59. A potentiometer, connected between a dc supply voltage V_{CC} and ground, is used to bias the

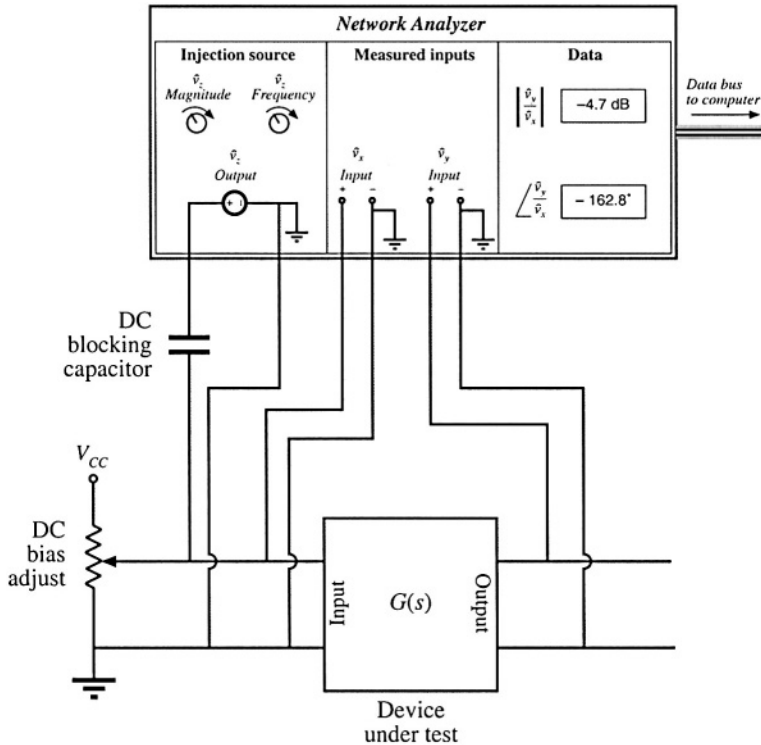


Fig. 8.59 Measurement of a transfer function.

amplifier input to attain the correct quiescent operating point. The injection source voltage \hat{v}_z is coupled to the amplifier input terminals via a dc blocking capacitor. This blocking capacitor prevents the injection voltage source from upsetting the dc bias. The network analyzer inputs \hat{v}_x and \hat{v}_y are connected to the input and output terminals of the amplifier. Hence, the measured transfer function is

$$\frac{\hat{v}_y(s)}{\hat{v}_x(s)} = G(s) \quad (8.177)$$

Note that the blocking capacitance, bias potentiometer, and \hat{v}_z amplitude have no effect on the measured transfer function

An impedance

$$Z(s) = \frac{\hat{v}(s)}{\hat{i}(s)} \quad (8.178)$$

can be measured by treating the impedance as a transfer function from current to voltage. For example, measurement of the output impedance of an amplifier is illustrated in Fig. 8.60. The quiescent operating condition is again established by a potentiometer which biases the amplifier input. The injection source \hat{v}_z is coupled to the amplifier output through a dc blocking capacitor. The injection source voltage \hat{v}_z excites a current \hat{i}_{out} in impedance Z_s . This current flows into the output of the amplifier, and excites a

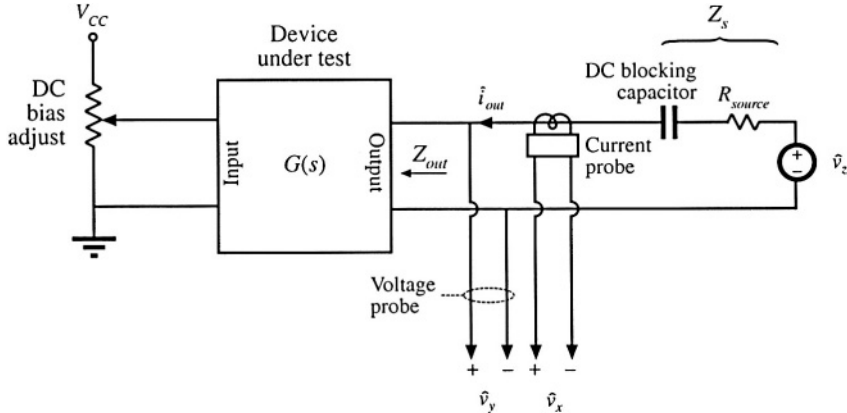


Fig. 8.60 Measurement of the output impedance of a circuit.

voltage across the amplifier output impedance:

$$Z_{out}(s) = \left. \frac{\hat{v}_y(s)}{\hat{i}_{out}(s)} \right|_{\substack{\text{amplifier} \\ \text{ac input}}} = 0 \quad (8.179)$$

A current probe is used to measure \hat{i}_{out} . The current probe produces a voltage proportional to \hat{i}_{out} ; this voltage is connected to the network analyzer input \hat{v}_x . A voltage probe is used to measure the amplifier output voltage \hat{v}_y . The network analyzer displays the transfer function \hat{v}_y/\hat{v}_x , which is proportional to Z_{out} . Note that the value of Z_s and the amplitude of \hat{v}_z do not affect the measurement of Z_{out} .

In power applications, it is sometimes necessary to measure impedances that are very small in magnitude. Grounding problems[4] cause the test setup of Fig. 8.60 to fail in such cases. The reason is illustrated in Fig. 8.61 (a). Since the return connections of the injection source \hat{v}_z and the analyzer input \hat{v}_y are both connected to earth ground, the injected current \hat{i}_{out} can return to the source through the return connections of either the injection source or the voltage probe. In practice, \hat{i}_{out} divides between the two paths according to their relative impedances. Hence, a significant current $(1 - k)\hat{i}_{out}$ flows through the return connection of the voltage probe. If the voltage probe return connection has some total contact and wiring impedance Z_{probe} , then the current induces a voltage drop $(1 - k)\hat{i}_{out}Z_{probe}$ in the voltage probe wiring, as illustrated in Fig. 8.61(a). Hence, the network analyzer does not correctly measure the voltage drop across the impedance Z . If the internal ground connections of the network analyzer have negligible impedance, then the network analyzer will display the following impedance:

$$Z + (1 - k)Z_{probe} = Z + Z_{probe}\parallel Z_{rz} \quad (8.180)$$

Here, Z_{rz} is the impedance of the injection source return connection. So to obtain an accurate measurement, the following condition must be satisfied:

$$\|Z\| \gg \|(Z_{probe}\parallel Z_{rz})\| \quad (8.181)$$

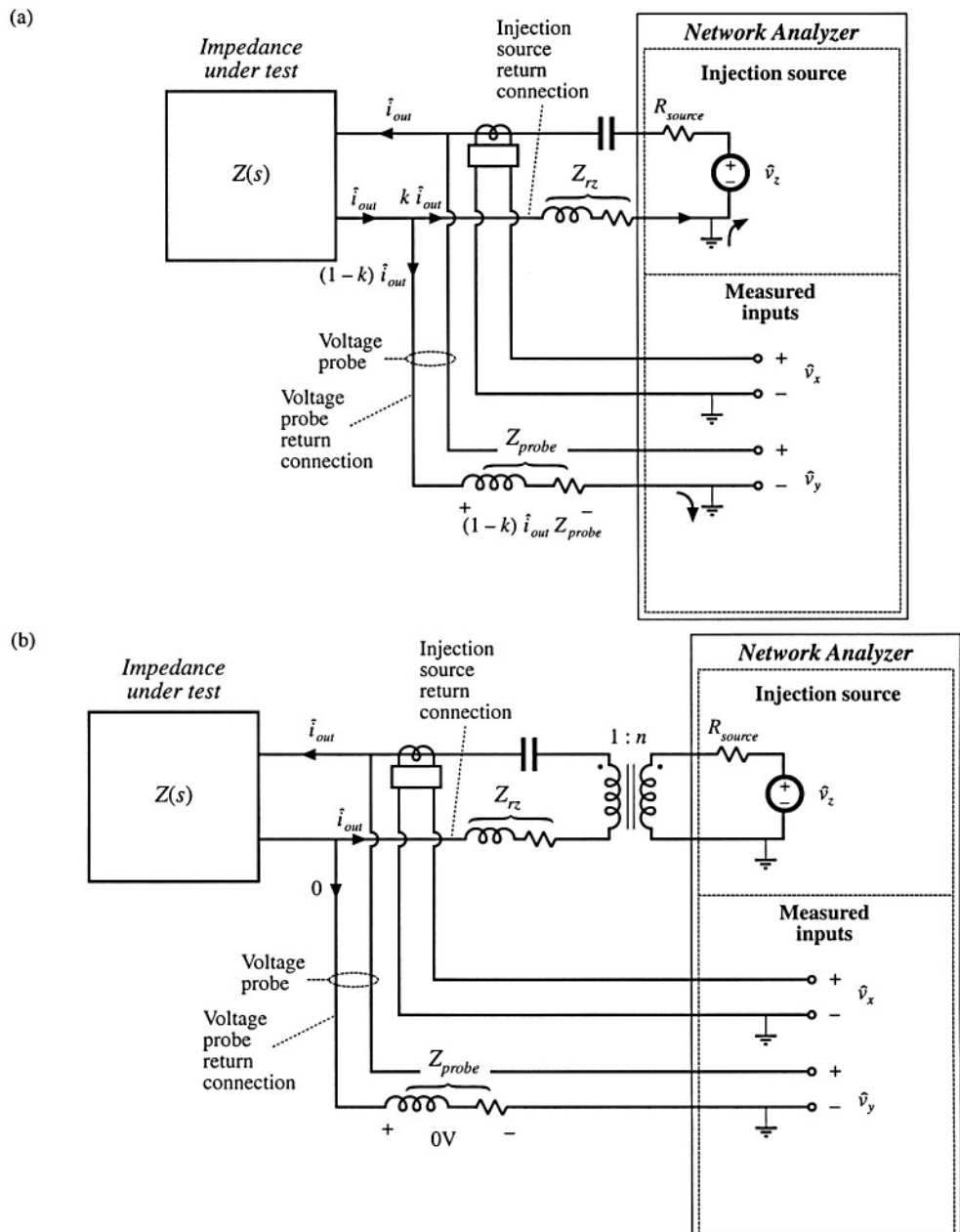


Fig. 8.61 Measurement of a small impedance $Z(s)$: (a) current flowing in the return connection of the voltage probe induces a voltage drop that corrupts the measurement; (b) an improved experiment, incorporating isolation of the injection source.

A typical lower limit on $\| Z \|$ is a few tens or hundreds of milliohms.

An improved test setup for measurement of small impedances is illustrated in Fig. 8.61(b). An isolation transformer is inserted between the injection source and the dc blocking capacitor. The return connections of the voltage probe and injection source are no longer in parallel, and the injected current i_{out} must now return entirely through the injection source return connection. An added benefit is that the transformer turns ratio n can be increased, to better match the injection source impedance to the impedance under test. Note that the impedances of the transformer, of the blocking capacitor, and of the probe and injection source return connections, do not affect the measurement. Much smaller impedances can therefore be measured using this improved approach.

8.6 SUMMARY OF KEY POINTS

1. The magnitude Bode diagrams of functions which vary as $(f/f_0)^n$ have slopes equal to $20n$ dB per decade, and pass through 0 dB at $f = f_0$.
2. It is good practice to express transfer functions in normalized pole-zero form; this form directly exposes expressions for the salient features of the response, that is, the corner frequencies, reference gain, etc.
3. The right half-plane zero exhibits the magnitude response of the left half-plane zero, but the phase response of the pole.
4. Poles and zeroes can be expressed in frequency-inverted form, when it is desirable to refer the gain to a high-frequency asymptote.
5. A two-pole response can be written in the standard normalized form of Eq. (8.58). When $Q > 0.5$, the poles are complex conjugates. The magnitude response then exhibits peaking in the vicinity of the corner frequency, with an exact value of Q at $f = f_0$. High Q also causes the phase to change sharply near the corner frequency.
6. When Q is less than 0.5, the two pole response can be plotted as two real poles. The low- Q approximation predicts that the two poles occur at frequencies f_0/Q and Qf_0 . These frequencies are within 10% of the exact values for $Q \leq 0.3$.
7. The low- Q approximation can be extended to find approximate roots of an arbitrary degree polynomial. Approximate analytical expressions for the salient features can be derived. Numerical values are used to justify the approximations.
8. Salient features of the transfer functions of the buck, boost, and buck-boost converters are tabulated in Section 8.2.2. The line-to-output transfer functions of these converters contain two poles. Their control-to-output transfer functions contain two poles, and may additionally contain a right half-plane zero.
9. Approximate magnitude asymptotes of impedances and transfer functions can be easily derived by graphical construction. This approach is a useful supplement to conventional analysis, because it yields physical insight into the circuit behavior, and because it exposes suitable approximations. Several examples, including the impedances of basic series and parallel resonant circuits and the transfer function $H(s)$ of the voltage divider circuit, are worked in Section 8.3. The input impedance, output impedance, and transfer functions of the buck converter are constructed in Section 8.4, and physical origins of the asymptotes, corner frequencies, and Q -factor are found.
10. Measurement of transfer functions and impedances using a network analyzer is discussed in Section 8.5. Careful attention to ground connections is important when measuring small impedances.

REFERENCES

- [1] R.D. MIDDLEBROOK, "Low Entropy Expressions: The Key to Design-Oriented Analysis," *IEEE Frontiers in Education Conference*, 1991 Proceedings, pp. 399-403, Sept. 1991.
- [2] R. D. MIDDLEBROOK, "Methods of Design-Oriented Analysis: The Quadratic Equation Revisited," *IEEE Frontiers in Education Conference*, 1992 Proceedings, pp. 95-102, Nov. 1991.
- [3] F. BARZEGAR, S. ĆUK, and R. D. MIDDLEBROOK, "Using Small Computers to Model and Measure Magnitude and Phase of Regulator Transfer Functions and Loop Gain," *Proceedings of Powercon 8*, April 1981. Also in *Advances in Switched-Mode Power Conversion*, Irvine: Teslaco, Vol. 1, pp. 251-278, 1981.
- [4] H. W. OTT, *Noise Reduction Techniques in Electronic Systems*, 2nd edit., New York: John Wiley & Sons, 1988, Chapter 3.

PROBLEMS

- 8.1** Express the gains represented by the asymptotes of Figs. 8.62(a) to (c) in factored pole-zero form. You may assume that all poles and zeroes have negative real parts.

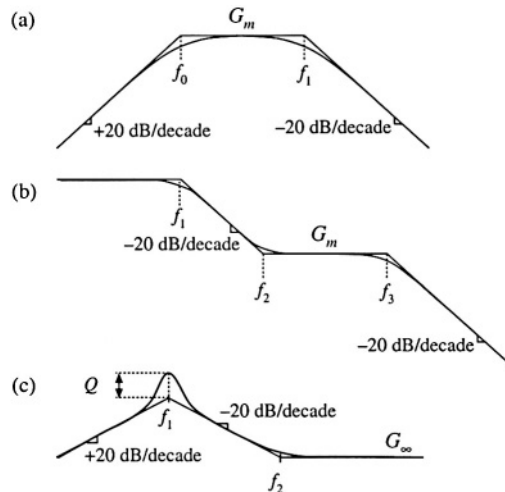


Fig. 8.62 Gain asymptotes for Problem 8.1.

- 8.2** Express the gains represented by the asymptotes of Figs. 8.63(a) to (c) in factored pole-zero form. You may assume that all poles and zeroes have negative real parts.
- 8.3** Derive analytical expressions for the low-frequency asymptotes of the magnitude Bode plots shown in Fig. 8.63(a) to (c).
- 8.4** Derive analytical expressions for the three magnitude asymptotes of Fig. 8.16.

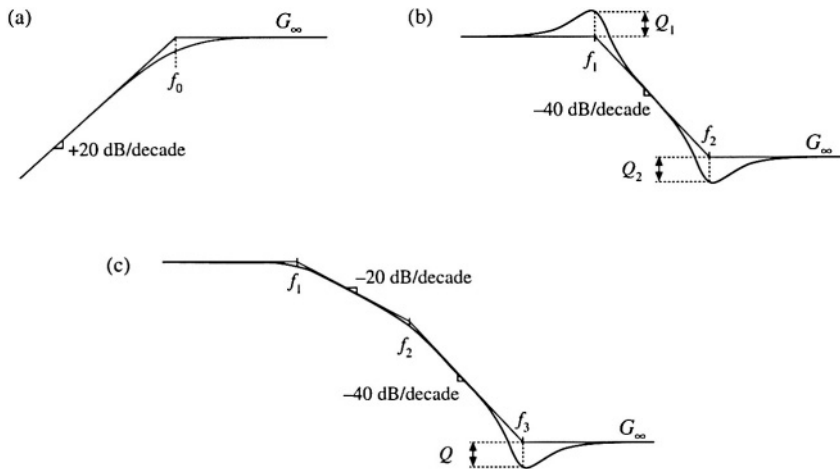


Fig. 8.63 Gain asymptotes for Problems 8.2 and 8.3.

8.5

An experimentally measured transfer function. Figure 8.64 contains experimentally measured magnitude and phase data for the gain function $A(s)$ of a certain amplifier. The object of this problem is to find an expression for $A(s)$. Overlay asymptotes as appropriate on the magnitude and phase data, and hence deduce numerical values for the gain asymptotes and corner frequencies of $A(s)$. Your magnitude and

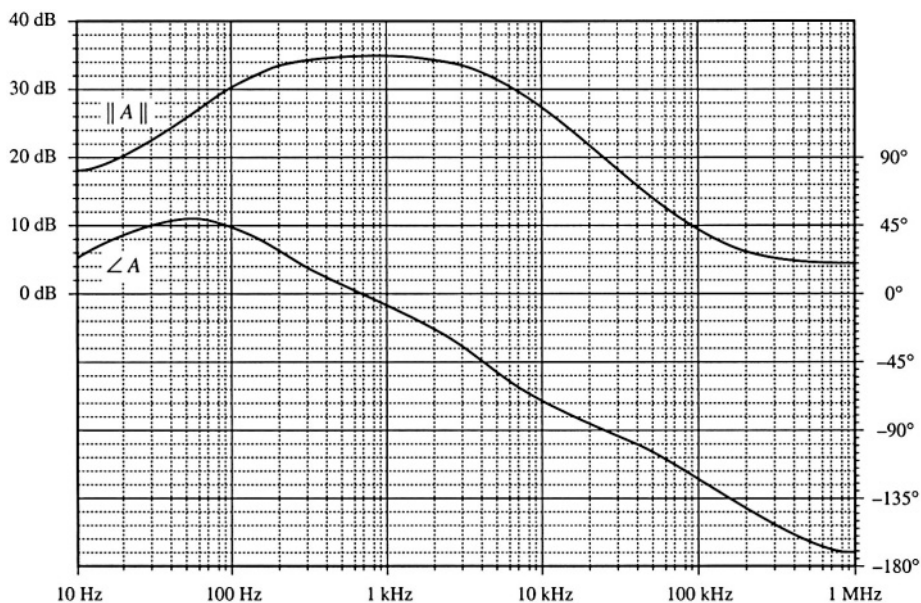


Fig. 8.64 Experimentally-measured magnitude and phase data, Problem 8.5.

phase asymptotes must, of course, follow all of the rules: magnitude slopes must be multiples of ± 20 dB per decade, phase slopes for real poles must be multiples of $\pm 45^\circ$ per decade, etc. The phase and magnitude asymptotes must be consistent with each other.

It is suggested that you start by guessing $A(s)$ based on the magnitude data. Then construct the phase asymptotes for your guess, and compare them with the given data. If there are discrepancies, then modify your guess accordingly and redo your magnitude and phase asymptotes. You should turn in: (1) your analytical expression for $A(s)$, with numerical values given, and (2) a copy of Fig. 8.64, with your magnitude and phase asymptotes superimposed and with all break frequencies and slopes clearly labeled.

- 8.6** An experimentally-measured impedance. Figure 8.65 contains experimentally measured magnitude and phase data for the driving-point impedance $Z(s)$ of a passive network. The object of this problem is to find an expression for $Z(s)$. Overlay asymptotes as appropriate on the magnitude and phase data, and hence deduce numerical values for the salient features of the impedance function. You should turn in: (1) your analytical expression for $Z(s)$, with numerical values given, and (2) a copy of Fig. 8.65, with your magnitude and phase asymptotes superimposed and with all salient features and asymptote slopes clearly labeled.

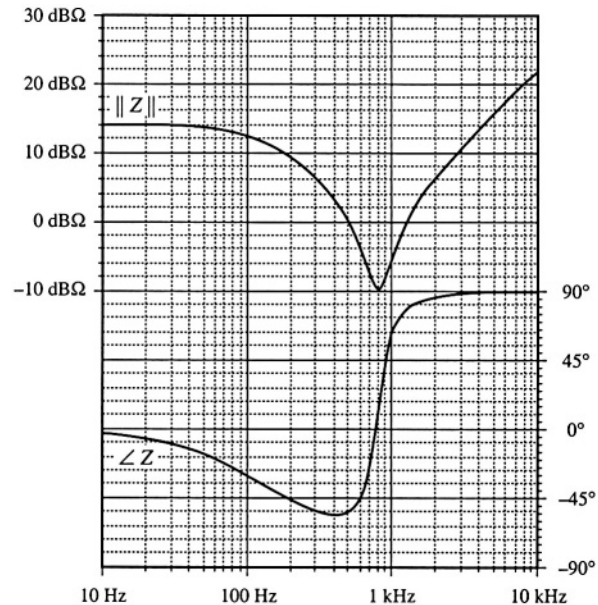


Fig. 8.65 Impedance magnitude and phase data, Problem 8.6.

- 8.7** In Section 7.2.9, the small-signal ac model of a nonideal flyback converter is derived, with the result illustrated in Fig. 7.27. Construct a Bode plot of the magnitude and phase of the converter output impedance $Z_{out}(s)$. Give both analytical expressions and numerical values for all important features in your plot. Note: $Z_{out}(s)$ includes the load resistance R . The element values are: $D = 0.4$, $n = 0.2$, $R = 6 \Omega$, $L = 600 \mu\text{H}$, $C = 100 \mu\text{F}$, $R_{on} = 5 \Omega$.
- 8.8** For the nonideal flyback converter modeled in Section 7.2.9:
- Derive analytical expressions for the control-to-output and line-to-output transfer functions $G_{vd}(s)$ and $G_{vg}(s)$. Express your results in standard normalized form.
 - Derive analytical expressions for the salient features of these transfer functions.
 - Construct the magnitude and phase Bode plots of the control-to-output transfer function, using

the following values: $n = 2$, $V_g = 48$ V, $D = 0.3$, $R = 5 \Omega$, $L = 250 \mu\text{H}$, $C = 100 \mu\text{F}$, $R_{on} = 1.2 \Omega$. Label the numerical values of the constant asymptotes, all corner frequencies, the Q -factor, and asymptote slopes.

- 8.9** Magnitude Bode diagram of an $R-L-C$ filter circuit. For the filter circuit of Fig. 8.66, construct the Bode plots for the magnitudes of the Thevenin-equivalent output impedance Z_{out} and the transfer function $H(s) = v_2/v_1$. Plot your results on semilog graph paper. Give approximate analytical expressions and numerical values for the important corner frequencies and asymptotes. Do all of the elements significantly affect Z_{out} and H ?

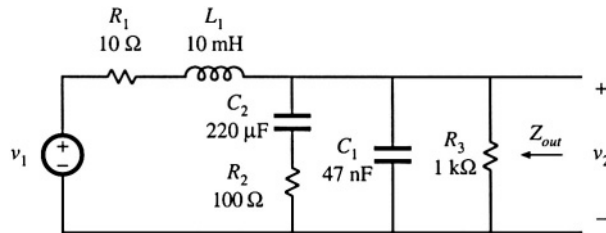


Fig. 8.66 Filter circuit of Problem 8.9.

- 8.10** Operational amplifier filter circuit. The op amp circuit shown in Fig. 8.67 is a practical realization of what is known as a *PID controller*, and is sometimes used to modify the loop gain of feedback circuits to improve their performance. Using semilog graph paper, sketch the Bode diagram of the magnitude of the transfer function $v_2(s)/v_1(s)$ of the circuit shown. Label all corner frequencies, flat asymptote gains, and asymptote slopes, as appropriate, giving both analytical expressions and numerical values. You may assume that the op amp is ideal.

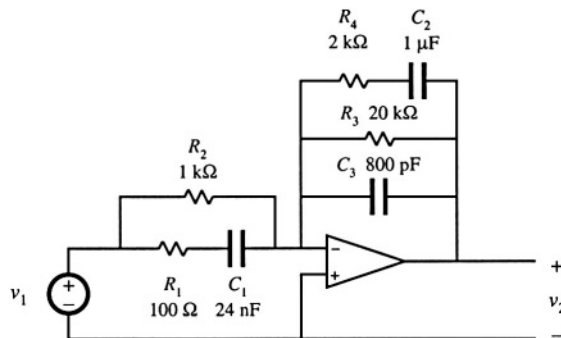


Fig. 8.67 Op-amp PID controller circuit, Problem 8.10.

- 8.11** Phase asymptotes. Construct the phase asymptotes for the transfer function $v_2(s)/v_1(s)$ of Problem 8.10. Label all break frequencies, flat asymptotes, and asymptote slopes.

- 8.12** Construct the Bode diagram for the magnitude of the output impedance Z_{out} of the network shown in Fig. 8.68. Give suitable analytical expressions for each asymptote, corner frequency, and Q -factor, as appropriate. Justify any approximations that you use.
The component values are:

$$\begin{array}{ll} L_1 = 100 \mu\text{H} & L_2 = 16 \text{ mH} \\ C_1 = 1000 \mu\text{F} & C_2 = 10 \mu\text{F} \\ R_1 = 5 \Omega & R_2 = 50 \Omega \end{array}$$

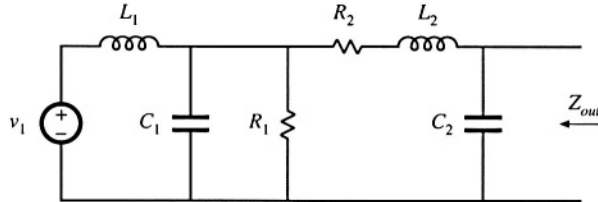


Fig. 8.68 Filter network of Problem 8.12.

- 8.13** The two section input filter in the circuit of Fig. 8.69 should be designed such that its output impedance $Z_{out}|_{v_g = 0}$ meets certain input filter design criteria, and hence it is desirable to construct the Bode plot for the magnitude of Z_s . Although this filter contains six reactive elements, $\|Z_s\|$ can nonetheless be constructed in a relatively straightforward manner using graphical construction techniques. The element values are:

$$\begin{array}{ll} L_1 = 32 \text{ mH} & C_1 = 32 \mu\text{F} \\ L_2 = 400 \mu\text{H} & C_2 = 6.8 \mu\text{F} \\ L_3 = 800 \mu\text{H} & R_1 = 10 \Omega \\ L_4 = 1 \mu\text{H} & R_2 = 1 \Omega \end{array}$$

- (a) Construct $\|Z_s\|$ using the “algebra on the graph” method. Give simple approximate analytical expressions for all asymptotes and corner frequencies.
 (b) It is desired that $\|Z_s\|$ be approximately equal to 5Ω at 500 Hz and 2.5Ω at 1 kHz. Suggest a simple way to accomplish this by changing the value of one component.

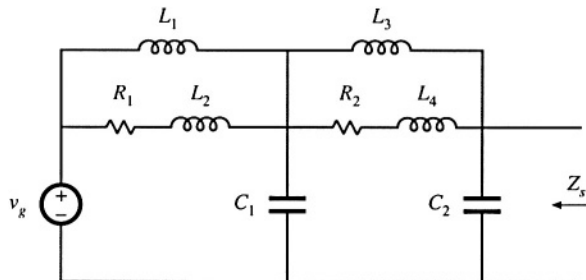


Fig. 8.69 Input filter circuit of Problem 8.13.

- 8.14** Construct the Bode plot of the magnitude of the output impedance of the filter illustrated in Fig. 8.70. Give approximate analytical expressions for each corner frequency. No credit will be given for computer-generated plots.
8.15 A certain open-loop buck-boost converter contains an input filter. Its small-signal ac model is shown in Fig. 8.71, and the element values are specified below. Construct the Bode plot for the magnitude of the converter output impedance $\|Z_{out}(s)\|$. Label the values of all important corner frequencies and asymptotes.

$$\begin{array}{ll} D = 0.6 & L_f = 150 \mu\text{H} \\ R = 6 \Omega & C_f = 16 \mu\text{F} \\ C = 0.33 \mu\text{F} & C_b = 2200 \mu\text{F} \\ L = 25 \mu\text{H} & R_f = 1 \Omega \end{array}$$

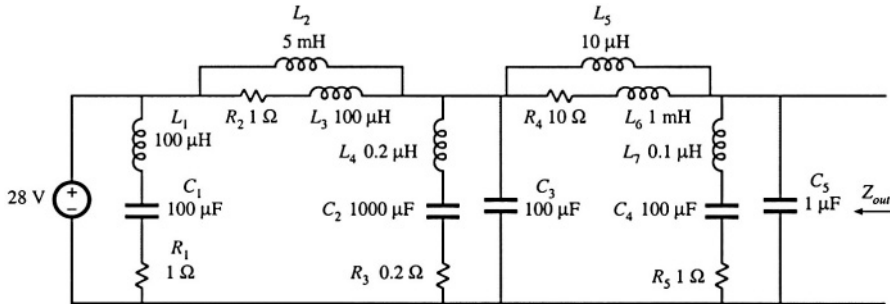


Fig. 8.70 Input filter circuit of Problem 8.14.

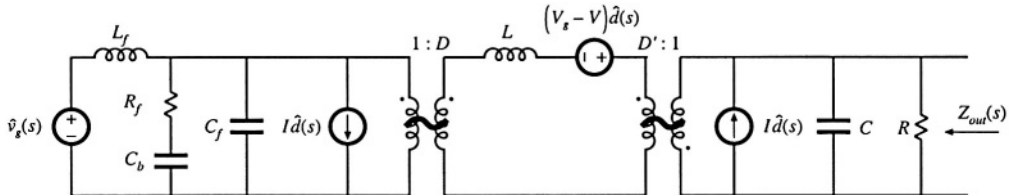


Fig. 8.71 Small-signal model of a buck-boost converter with input filter, Problem 8.15.

- 8.16** The small-signal equations of the Watkins-Johnson converter operating in continuous conduction mode are:

$$\begin{aligned} L \frac{d\hat{i}(t)}{dt} &= -D\hat{v}(t) + (2V_g - V)\hat{d}(t) + (D - D')\hat{v}_g(t) \\ C \frac{d\hat{v}(t)}{dt} &= D\hat{i}(t) - \frac{\hat{v}(t)}{R} \\ \hat{i}_g(t) &= (D - D')\hat{i}(t) + 2I\hat{d}(t) \end{aligned}$$

- (a) Derive analytical expressions for the line-to-output transfer function $G_{vg}(s)$ and the control-to-output transfer function $G_{vd}(s)$.
- (b) Derive analytical expressions for the salient features (dc gains, corner frequencies, and Q -factors) of the transfer functions $G_{vg}(s)$ and $G_{vd}(s)$. Express your results as functions of V_g , D , R , L , and C .
- (c) The converter operates at $V_g = 28 \text{ V}$, $D = 0.25$, $R = 28 \Omega$, $C = 100 \mu\text{F}$, $L = 400 \mu\text{H}$. Sketch the Bode diagram of the magnitude and phase of $G_{vd}(s)$. Label salient features.

- 8.17** The element values in the buck converter of Fig. 7.68 are:

$V_g = 120 \text{ V}$	$D = 0.6$
$R = 10 \Omega$	$R_g = 2 \Omega$
$L = 550 \mu\text{H}$	$C = 100 \mu\text{F}$

- (a) Determine an analytical expression for the control-to-output transfer function $G_{vg}(s)$ of this converter.
- (b) Find analytical expressions for the salient features of $G_{vg}(s)$.
- (c) Construct magnitude and phase asymptotes for G_{vg} . Label the numerical values of all slopes and

other important features.

8.18

Loss mechanisms in capacitors, such as dielectric loss and contact and foil resistance, can be modeled electrically using an *equivalent series resistance* (esr). Capacitors whose dielectric materials exhibit a high dielectric constant, such as electrolytic capacitors, tantalum capacitors, and some types of multi-layer ceramic capacitors, typically exhibit relatively high esr.

A buck converter contains a 1.6 mH inductor, and operates with a quiescent duty cycle of 0.5. Its output capacitor can be modeled as a $16 \mu\text{F}$ capacitor in series with a 0.2Ω esr. The load resistance is 10Ω . The converter operates in continuous conduction mode. The quiescent input voltage is $V_g = 120 \text{ V}$.

- (a) Determine an analytical expression for the control-to-output transfer function $G_{vg}(s)$ of this converter.
- (b) Find analytical expressions for the salient features of $G_{vg}(s)$.
- (c) Construct magnitude and phase asymptotes for G_{vg} . Label the numerical values of all slopes and other important features.

8.19

The LCC resonant inverter circuit contains the following transfer function:

$$H(s) = \frac{sC_1R}{1 + sR(C_1 + C_2) + s^2LC_1 + s^3LC_1C_2R}$$

- (a) When C_1 is sufficiently large, this transfer function can be expressed as an inverted pole and a quadratic pole pair. Derive analytical expressions for the corner frequencies and Q -factor in this case, and sketch typical magnitude asymptotes. Determine analytical conditions for validity of your approximation.
- (b) When C_2 is sufficiently large, the transfer function can be also expressed as an inverted pole and a quadratic pole pair. Derive analytical expressions for the corner frequencies and Q -factor in this case, and sketch typical magnitude asymptotes. Determine analytical conditions for validity of your approximation in this case.
- (c) When $C_1 = C_2$ and when the quadratic poles have sufficiently high Q , then the transfer function can again be expressed as an inverted pole and a quadratic pole pair. Derive analytical expressions for the corner frequencies and Q -factor in this case, and sketch typical magnitude asymptotes. Determine analytical conditions for validity of your approximation in this case.

8.20

A two-section $L-C$ filter has the following transfer function:

$$G(s) = \frac{1}{1 + s\left(\frac{L_1 + L_2}{R}\right) + s^2\left(L_1(C_1 + C_2) + L_2C_2\right) + s^3\left(\frac{L_1L_2C_1}{R}\right) + s^4\left(L_1L_2C_1C_2\right)}$$

The element values are:

$$R = 50 \text{ m}\Omega$$

$$C_1 = 680 \mu\text{F}$$

$$C_2 = 4.7 \mu\text{F}$$

$$L_1 = 500 \mu\text{H}$$

$$L_2 = 50 \mu\text{H}$$

- (a) Factor $G(s)$ into approximate real and quadratic poles, as appropriate. Give analytical expressions for the salient features. Justify your approximation using the numerical element values.
- (b) Construct the magnitude and phase asymptotes of $G(s)$.
- (c) It is desired to reduce the Q to 2, without significantly changing the corner frequencies or other features of the response. It is possible to do this by changing only two element values. Specify how to accomplish this.

8.21

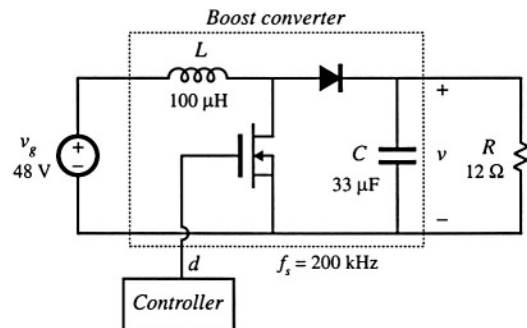
The boost converter of Fig. 8.72 operates in the continuous conduction mode, with quiescent duty cycle

$D = 0.6$. On semi-log axes, construct the magnitude and phase Bode plots of

- (a) the control-to-output transfer function $G_{vd}(s)$,
- (b) the line-to-output transfer function $G_{vg}(s)$,
- (c) the output impedance $Z_{out}(s)$, and
- (d) the input impedance $Z_{in}(s)$.

On each plot, label the corner frequencies and asymptotes.

Fig. 8.72 Boost converter of Problem 8.21.



8.22

The forward converter of Fig. 8.73 operates in the continuous conduction mode, with the quiescent values $V_g = 380 \text{ V}$ and $V = 28 \text{ V}$. The transformer turns ratio is $n_1/n_3 \approx 4.5$. On semi-log axes, construct the magnitude and phase Bode plots of

- (a) the control-to-output transfer function $G_{vd}(s)$, and
- (b) the line-to-output transfer function $G_{vg}(s)$.

On each plot, label the corner frequencies and asymptotes. Hint: other than introduction of the turns ratio n_1/n_3 , the transformer does not significantly affect the small-signal behavior of the forward converter.

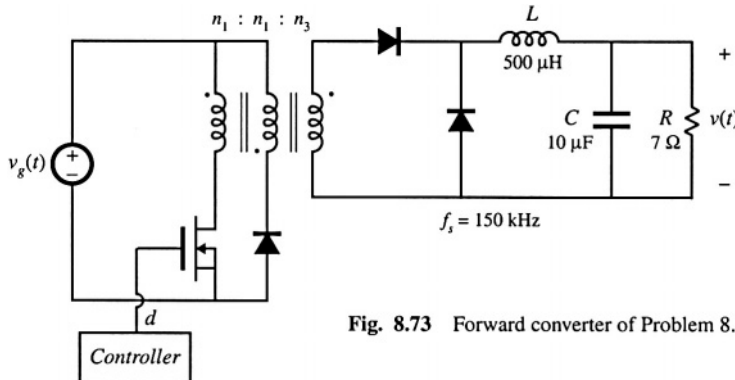


Fig. 8.73 Forward converter of Problem 8.22.

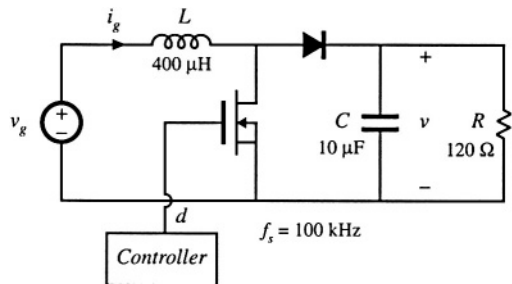
8.23

The boost converter of Fig. 8.74 operates in the continuous conduction mode, with the following quiescent values: $V_g = 120 \text{ V}$, $V = 300 \text{ V}$. It is desired to control the converter input current waveform, and hence it is necessary to determine the small-signal transfer function

$$G_{id}(s) = \left. \frac{\hat{i}_g(s)}{\hat{d}(s)} \right|_{\hat{v}_g(s)=0}$$

- (a) Derive an analytical expression for $G_{id}(s)$. Express all poles and zeroes in normalized standard form, and give analytical expressions for the corner frequencies, Q -factor, and dc gain.
- (b) On semi-log axes, construct the Bode plot for the magnitude and phase of $G_{id}(s)$.

Fig. 8.74 Boost converter of Problem 8.23.



- 8.24** The buck-boost converter of Fig. 8.75 operates in the continuous conduction mode, with the following quiescent values: $V_g = 48$ V, $V = -24$ V. On semi-log axes, construct the magnitude and phase Bode plots of:

- (a) the control-to-output transferfunction $G_{vo}(s)$, and
 (b) the output impedance $Z_{out}(s)$.

On each plot, label the corner frequencies and asymptotes as appropriate.

Fig. 8.75 Buck-boost converter of Problem 8.24.

